

Multi-colour photometry and Gaia EDR3 astrometry of two couples of binary clusters (NGC 5617 and Trumpler 22) and (NGC 3293 and NGC 3324).

D. Bisht^{1,*}, Qingfeng Zhu¹, R. K. S. Yadav², Shashikiran Ganesh³, Geeta Rangwal⁴, Alok Durgapal⁴, Devesh P. Saria⁵, Ing-Guey Jiang⁵

¹ Key Laboratory for Researches in Galaxies and Cosmology, University of Science and Technology of China, Chinese Academy of Sciences, Hefei, Anhui, 230026, China

² Aryabhata Research Institute of Observational Sciences, Manora Peak, Nainital 263129, India

³ Physical Research Laboratory, Ahmedabad 380009, India

⁴ Center of Advanced Study, Department of physics, D.S.B. campus, Kumaun University, Nainital, 263002, India

⁵ Department of Physics and Institute of Astronomy, National Tsing-Hua University, Hsin-Chu, Taiwan

Accepted Received; in original form

ABSTRACT

This paper presents a comprehensive analysis of two pairs of binary clusters (NGC 5617 and Trumpler 22) and (NGC 3293 and NGC 3324) located in the fourth quadrant of our Galaxy. For this purpose we use different data taken from VVV survey, WISE, VPHAS, APASS, GLIMPSE along with Gaia EDR3 astrometric data. We identified 584, 429, 692 and 273 most probable cluster members with membership probability higher than 80% towards the region of clusters NGC 5617, Trumpler 22, NGC 3293 and NGC 3324. We estimated the value of $R = \frac{A_V}{E(B-V)}$ as ~ 3.1 for clusters NGC 5617 and Trumpler 22, which indicates normal extinction law. The value of $R \sim 3.8$ and ~ 1.9 represent the abnormal extinction law towards the clusters NGC 3293 and NGC 3324. Our Kinematical analysis show that all these clusters have circular orbits. Ages are found to be 90 ± 10 and 12 ± 3 Myr for the cluster pairs (NGC 5617 and Trumpler 22) and (NGC 3293 and NGC 3324), respectively. The distances of 2.43 ± 0.08 , 2.64 ± 0.07 , 2.59 ± 0.1 and 2.80 ± 0.2 kpc estimated using parallax are alike to the values calculated by using the distance modulus. We have also identified 18 and 44 young stellar object candidates present in NGC 5617 and Trumpler 22, respectively. Mass function slopes are found to be in fair agreement with the Salpeter's value. The dynamical study of these objects shows a lack of faint stars in their inner regions, which leads to the mass-segregation effect. Our study indicates that NGC 5617 and Trumpler 22 are dynamically relaxed but the other pair of clusters are not. Orbital alongwith the physical parameters show that the clusters in both pairs are physically connected.

Key words: Open clusters: individual: NGC 5617, Trumpler 22, NGC 3293, NGC 3324 - Galactic Orbits- Mass function- Mass segregation

1 INTRODUCTION

The open clusters (OCs) are considered excellent laboratories for studies of stellar evolution and the dynamics of stellar systems. The structure of the cluster is a result of its evolutionary processes such as initial physical conditions of the molecular clouds, external tidal perturbation, etc (Chen et al., 2004; Sharma et al., 2008). OCs become beneficial ob-

* E-mail: dbisht@ustc.edu.cn; zhuqf@ustc.edu.cn; shashikiran.ganesh@gmail.com; rkant@aries.res.in; alokdurgapal@gmail.com; geetarangwal91@gmail.com; deveshpath-sariya@gmail.com; jiang@phys.nthu.edu.tw

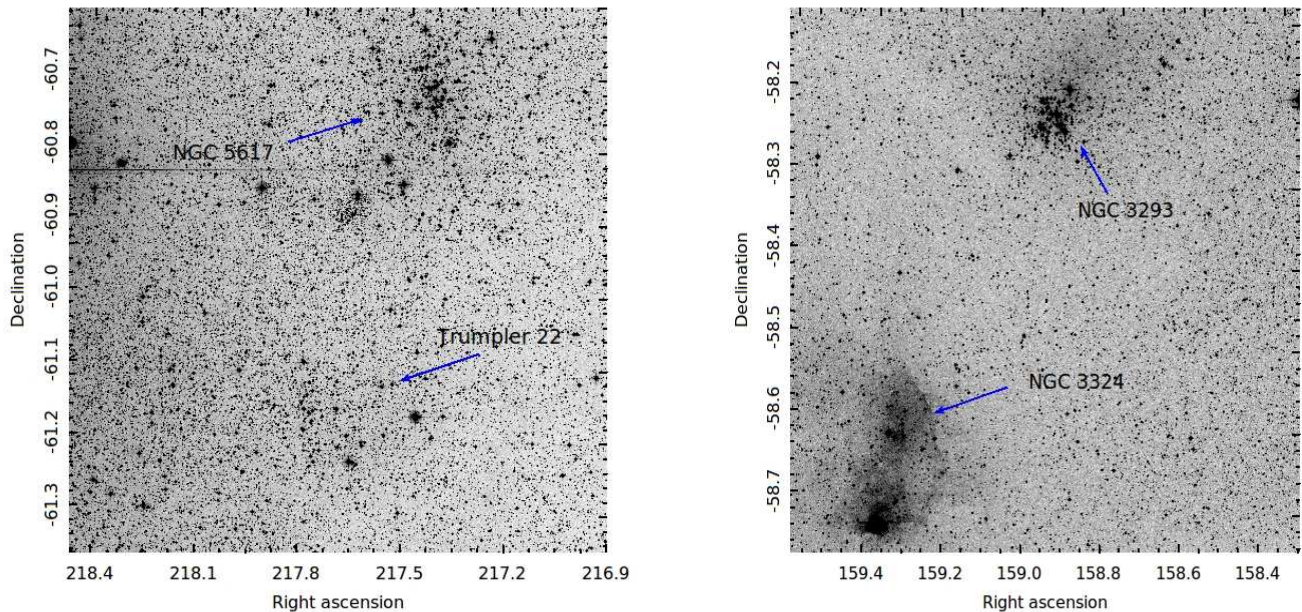


Figure 1. Identification maps of two pair of clusters (NGC 5617 and Trumpler 22) and (NGC 3293 and NGC 3324) as taken from the Digitized Sky Survey.

jects for the stellar evolution because they are formed by the collapse and fragmentation of a turbulent molecular cloud (Harris & Pudritz 1994; Bate et al. 2003). OCs are influenced by the contamination of field stars. In recent years, the detailed membership analysis of stars in the cluster field has become a subject of intense investigation, mainly in view to understand the cluster properties (Carraro et al., 2008; Yadav et al., 2008; Joshi et al., 2014; Cantat-Gaudin et al. 2018). Recently many authors have been estimated membership probability for clusters using Gaia DR2 kinematical data (Cantat-Gaudin et al. 2018, 2019; Castro-Ginard et al. 2018, 2019; Bisht et al. 2019, 2020). The (early) Third Gaia Data Release (hereafter EDR3; Gaia Collaboration et al. 2020) was made public on 3rd December 2020. EDR3 consists the central coordinates, proper motions in right ascension and declination and parallax angles (α , δ , $\mu_{\alpha \cos \delta}$, μ_{δ} , π) for around 1.46 billion sources with a limiting magnitude of 3 to 21 mag in *G* band. The Gaia EDR3 data are much accurate than second data release of Gaia mission.

Bhatia (1990) has suggested that the lifetime of binary clusters depends on cluster separation, tidal force of the parental Galaxy and encounters with giant molecular clouds. In the Large and Small Magellanic Clouds (LMC and SMC), $\sim 10\%$ of the well known OCs may be in pairs and around 50% of them are primordial binary clusters (Bhatia & Hatzidimitriou 1988; Dieball & Grebel 2000; Dieball, Muller & Grebel 2002). In our Milky Way Galaxy around 10 % of total OCs have been proposed to be in binary or multiple systems (Subramaniam et al. 1995; de la Fuente Marcos & le la Fuente Marcos 2010). The main aim of the paper is to study the properties of the binary open clusters NGC 5617, Trumpler 22 and NGC 3293, NGC 3324. The

available information about these objects in the literature are as follows-

NGC 5617: (C1426-605) ($\alpha_{2000} = 14^h 29^m 48^s$, $\delta_{2000} = -60^\circ 43' 00''$; $l=314^\circ 67$, $b=-0^\circ 11$). Lindoff (1968) has estimated age of the cluster as $\sim 4.6 \times 10^7$ yr using photographic data. Based on photographic-photoelectric photometry Haug (1978) obtained parameters for this cluster as; $E(B-V) = 0.53$, $A_V = 1.69$ and a distance of 1.8 Kpc. CCD *UBV* photometry has been reported by Kjeldsen & Frandsen (1991, hereafter KF91), who got a smaller reddening $E(B-V) = 0.48 \pm 0.02$, a larger distance of 2.05 ± 0.2 Kpc and an age of 70 Myr. It is an intermediate age open cluster (8.2×10^7 years) containing red giants and blue straggler stars (Ahumada & Lapasset 2007) in its surroundings, which membership of the cluster is still in doubt.

Trumpler 22: ($\alpha_{2000} = 14^h 31^m 02^s$, $\delta_{2000} = -61^\circ 10' 00''$; $l=314^\circ 64$, $b=-0^\circ 58$). Haug (1978) studied this object using photographic data. De Silva et al. (2015) has done photometric and spectroscopic analysis of both clusters NGC 5617 and Trumpler 22. He has obtained common age, distance and radial velocity for both clusters as 70 ± 10 Myr, 2.1 ± 0.3 Kpc and 38.5 ± 2.0 Km/sec respectively.

NGC 3293: ($\alpha_{2000} = 10^h 35^m 51^s$, $\delta_{2000} = -58^\circ 13' 48''$; $l=285^\circ 85$, $b=0^\circ 07$). This object is moderately younger and belongs to the rich Carina complex. Preibisch et al. (2017) studied this object using Chandra X-ray observations. They found the age of this object as 8-10 Myr. Delgado et al. (2011) have estimated parameters of pre-main sequence stars in this cluster. They obtained flatter mass function slope than the Salpeter's value. Slawson et al. (2007) studied the stellar mass spectrum of NGC 3293 using CCD *UBVRI* images. They found significantly fewer lower mass stars towards the region of NGC 3293. They confirmed the age of

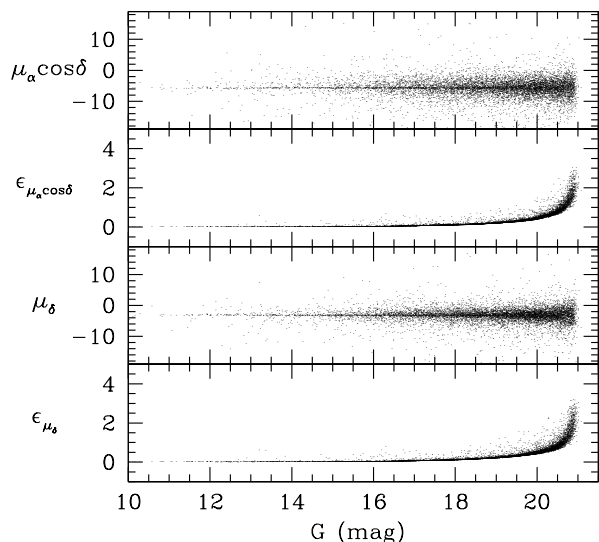


Figure 2. Plot of proper motions and their errors versus G magnitude for the cluster NGC 5617 is shown as an example.

this cluster as 10 Myr on the basis of the presence of some intermediate-mass stars near the main sequence in the HR diagram. Tuvikene & Sterken (2006) checked the variability of stars in NGC 3293. Out of 15 candidates they found 3 constant stars, 10 stars with significant variability while 2 of them were considered as suspected variables. Photometric study has been done by Baume et al. (2003) using CCD photometric observations at $UBVRI_C H_\alpha$. They found distance as 2750 ± 250 pc and age as 8 ± 1 Myr. The initial mass function slope was estimated as 1.2 ± 0.2 , a bit flatter than the typical slope for field stars.

NGC 3324: ($\alpha_{2000} = 10^h 37^m 20^s$, $\delta_{2000} = -58^\circ 38' 30''$; $l=286^\circ 23$, $b=-0^\circ 18$). This object is also situated in proximity with NGC 3293 in Carina complex. Carraro et al. (2001) reported the first CCD $UBVRI$ photometry of NGC 3324, and found that this cluster is very young and contains several pre-main sequence stars. Claria (1977) presented wide band (UBV) and narrow band (H_α) photometry of this object. According to this study, NGC 3324 contains at least twenty O- and B-type members and it is located at 3.12 kpc in the Carina spiral feature. A mean colour excess and age are found as 0.47 mag and 2.2×10^6 years, respectively.

Apart from this available information for the clusters under study, membership is still a question of debate. Our main goal is to estimate the membership probability for these objects and determine the more precise fundamental parameters, Galactic orbits, luminosity function, mass function and dynamical state of the clusters NGC 5617, Trumpler 22, NGC 3293 and NGC 3324 using multiwavelength photometric data along with high-precision astrometric data from the Gaia EDR3 catalog. Gaia EDR3 involves photometric magnitudes in three bands (G, G_{BP}, G_{RP}), astrometric data at the sub milliarcsecond level along with parallax values (Gaia Collaboration et al. 2020).

Proper motion is a very important parameter of open clusters. Another important implication of the cluster's

proper motion is the determination of membership probabilities for individual stars (Sanders 1971). The investigation of OCs also offers to understand the mass function (MF) of stellar objects, which is an important tool to study the star formation history (Sharma et al. 2017; Jose et al. 2017, and references therein). In recent years, many authors have estimated the present day MF for plenty of OCs (Dib et al. 2017; Joshi et al. 2020). The spatial distribution of massive and faint stars within the clusters provides important information to understand the mass-segregation in OCs (Bisht et al. 2016).

The outline of the paper is as follows. The brief description of the data used has been described in Section 2. Section 3 is devoted to the study of mean proper motion and estimation of membership probability of stars. In Section 4, orbits of the clusters are calculated. The cluster structure has been explained in Section 5. The main fundamental parameters of the clusters are discussed in Section 6. The dynamical properties of the clusters are described in Section 7. Binarity of clusters have been discussed in Section 8. The conclusion of this paper has been given in Section 9.

2 DATA USED

We collected the astrometric and photometric data from Gaia EDR3 along with broad-band photometric data from VVV, WISE, APASS, GLIMPSE, and VPHAS data for clusters NGC 5617, Trumpler 22, NGC 3293 and NGC 3324. The finding charts for the clusters are taken from Digitized Sky Survey (DSS) and shown in Fig. 1. We cross-matched each catalog for the clusters under study. The brief description has been given for each data sets as follows:

2.1 The multi-dimensional Gaia EDR3 data

We used Gaia EDR3 (Gaia Collaboration et al. 2020) data for the astrometric analysis of the clusters NGC 5617, Trumpler 22, NGC 3293 and NGC 3324. Data should be considered complete down to $G=18-19$ mag. The G, G_{BP} and G_{RP} bands cover the wavelength range from 330 to 1050 nm, 330-680 nm and 630-1050 nm, respectively (Evans et al. 2018). We have plotted the photometric errors in G, G_{BP} and G_{RP} versus G band as shown in the bottom panels of Fig. 3. The uncertainties in parallaxes have the range of $\sim 0.02-0.03$ milliarcsecond (mas) for sources at $G \leq 15$ mag and ~ 0.07 mas for sources with $G \sim 17$ mag. The uncertainties in the respective proper motion components are up to $0.01-0.02 \text{ mas yr}^{-1}$ (for $G \leq 15$ mag), 0.05 mas yr^{-1} (for $G \sim 17$ mag) and 0.4 mas yr^{-1} (for $G \sim 20$ mag). The proper motion and their corresponding errors are plotted against G magnitude in Fig. 2.

2.2 WISE data

This database is a NASA Medium Class Explorer mission that conducted a digital imaging survey of the entire sky in the mid-IR bands. The effective wavelength of mid-IR bands are $3.35 \mu\text{m}$ (W1), $4.60 \mu\text{m}$ (W2), $11.56 \mu\text{m}$ (W3) and $22.09 \mu\text{m}$ (W4) (Wright et al. 2010). We have taken data for clusters NGC 5617, Trumpler 22, NGC 3293 and NGC 3324 from the ALLWISE source catalog. This catalog has

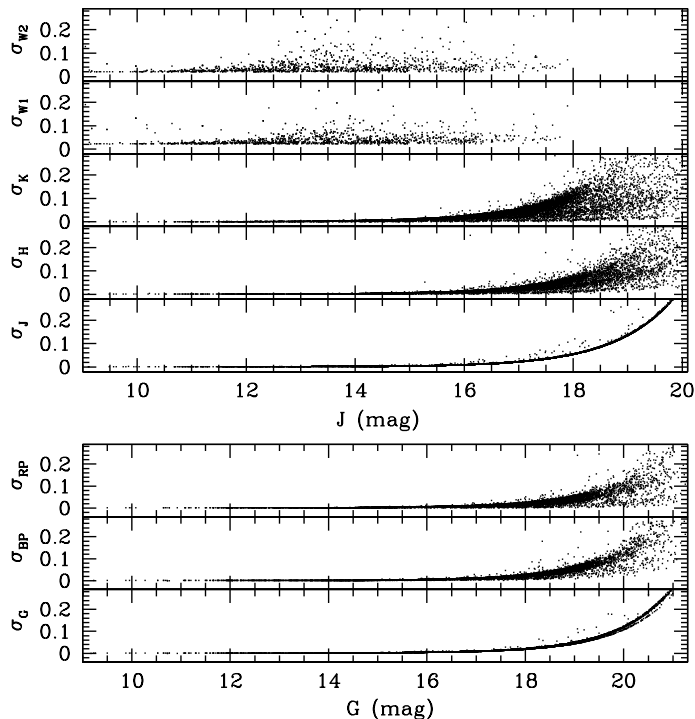


Figure 3. Photometric errors in Gaia pass bands G , G_{BP} and G_{RP} against G magnitude in three lower panels while photometric errors in J , H , K , W_1 and W_2 magnitudes against J magnitude in upper five panels.

achieved 5σ point source sensitivities better than 0.08, 0.11, 1 and 6 mJy at 3.35, 4.60, 11.56, and 22.09 μm , which is expected to be more than 99% of the sky (Bisht et al. 2020). These sensitivities are 16.5, 15.5, 11.2, and 7.9 for W_1 , W_2 , W_3 , and W_4 bands correspond to vega magnitudes.

2.3 VVV data

The VVV survey is an ESO infrared Large Public survey (Minniti et al. 2010; Saito et al. 2012b) which uses the 4-meter VISTA telescope located at Cerro Paranal Observatory, Chile. The effective wavelength of near-infrared broadband filters are 0.87 μm (Z), 1.02 μm (Y), 1.25 μm (J), 1.64 μm (H) and 2.14 μm (K). The telescope has a near-infrared camera, VIRCAM (Dalton et al. 2006), consisting of an array of 16 detectors with 2048 \times 2048 pixels. The errors given in the VVV catalog for the (J , H , K) bands and W_1 , W_2 bands from the WISE catalog are plotted against J magnitudes in the top panels of Fig. 3.

2.4 APASS data

The American Association of Variable Star Observers (AAVSO) Photometric All-Sky Survey (APASS) is organized in five filters: B , V (Landolt) and g' , r' , i' proving stars with V band magnitude range from 7 to 17 mag (Heden & Munari 2014). DR9 is the latest catalog and covers about 99% sky (Heden et al. 2016). We have extracted this data from <http://vizier.u-strasbg.fr/viz-bin/VizieR?source=II/3303> and NGC 3324. We made a catalog of common stars

2.5 GLIMPSE data

The Galactic Legacy Infrared Mid-Plane Survey Extraordinaire (GLIMPSE; Benjamin et al. 2003; Churchwell et al. 2004) data has been used for clusters NGC 5617 and Trumpler 22. The basic calibration of the GLIMPSE IRAC frames was performed by the Spitzer Science Center Pipeline (Spitzer Observers Manual 2004). This database consists only of high-reliability sources with each source must be detected twice in any of the four IRAC bands (3.6, 4.5 5.8, 8.0 μm).

2.6 VPHAS data

The VST/Omegacam Photometric H_α Survey (VPHAS) is imaging the entire Southern Milky Way in visible light at ~ 1 arcsec angular resolution down to ≥ 20 mag using the VLT Survey Telescope in Chile. We have extracted data from VPHAS catalog (Drew et al. 2014) for the analysis of clusters under study. This catalog includes data in u , g , r , i and H_α passbands.

3 MEAN PROPER MOTION AND CLUSTER MEMBERSHIP

The proper motion of stars is very precious to differentiate member stars from field stars. We have used proper motion and parallax data from the Gaia EDR3 catalog to remove field stars from the clusters NGC 5617, Trumpler 22, NGC

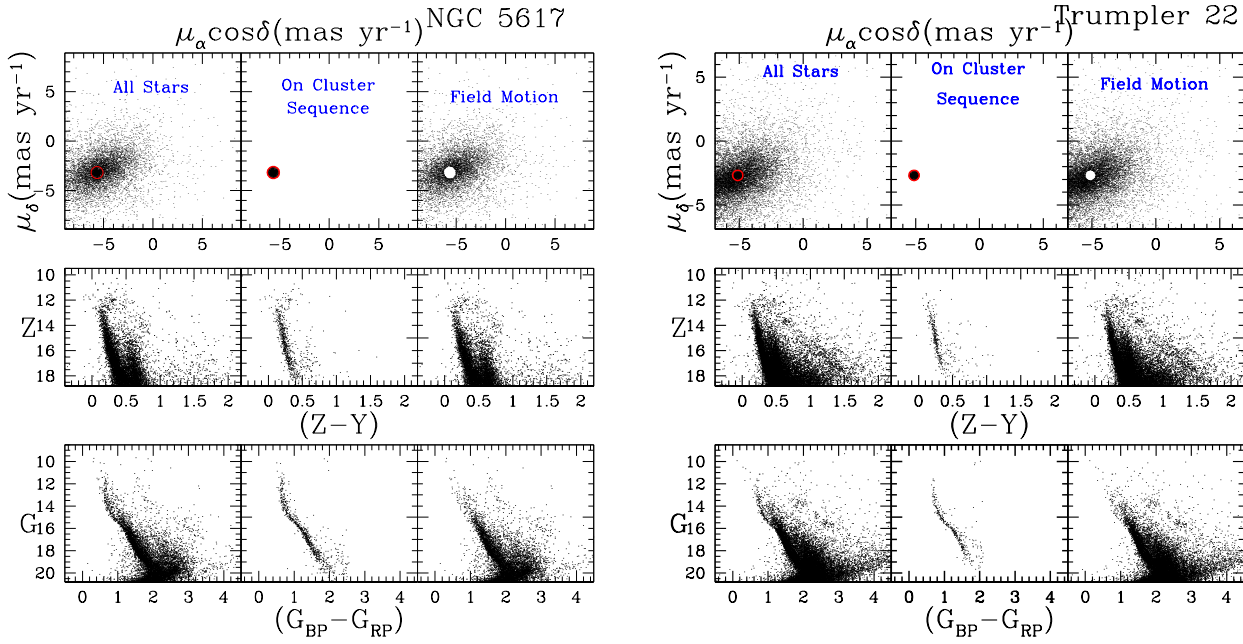


Figure 4. (Top panels) VPDs for clusters NGC 5617 and Trumpler 22. (Middle panels) Z versus $Z - Y$ colour magnitude diagrams. (Bottom panels) G versus $(G_{BP} - G_{RP})$ colour magnitude diagrams. For each cluster CMDs, (Left panel) The entire sample. (Center) Stars within the circle of 0.6 mas yr^{-1} and 0.4 mas yr^{-1} radius for clusters NGC 5617 and Trumpler 22 centered around the mean proper motion of the clusters. (Right) Probable background/foreground field stars in the direction of these clusters. All plots show only stars with PM error smaller than 0.4 mas yr^{-1} in each coordinate.

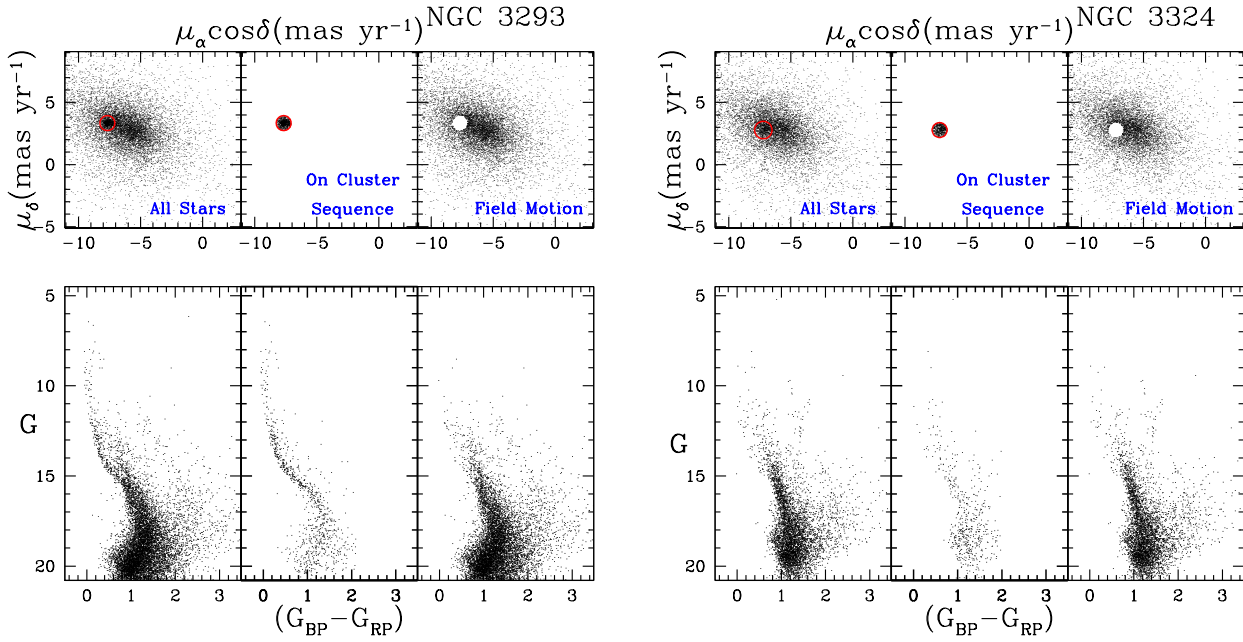


Figure 5. (Top panels) VPDs for clusters NGC 3293 and NGC 3324. (Bottom panels) G versus $(G_{BP} - G_{RP})$ colour magnitude diagrams. For each cluster CMDs, (Left panel) The entire sample. (Center) Stars within the circle of 0.6 mas yr^{-1} radius for clusters NGC 3293 and NGC 3324 centered around the mean proper motion of the clusters. (Right) Probable background/foreground field stars in the direction of these clusters. All plots show only stars with PM error smaller than 0.4 mas yr^{-1} in each coordinate.

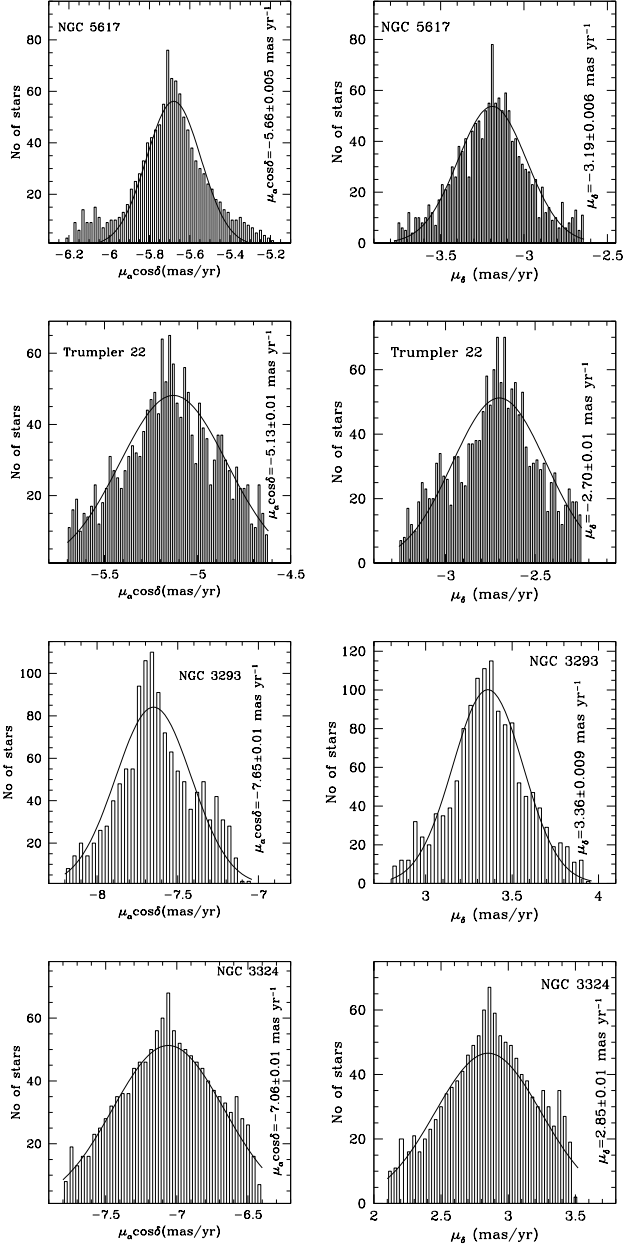


Figure 6. Proper motion histograms in 0.1 mas yr^{-1} bins in $\mu_\alpha \cos \delta$ and μ_δ of the clusters. The Gaussian function fit to the central bins provides the mean values in both directions as shown in each panel.

after matching the Gaia data with the above mentioned photometric data sets in this paper.

PMs, $\mu_\alpha \cos \delta$ and μ_δ are plotted as vector point diagrams (VPDs) in the top panels of Fig. 4 and Fig. 5 to see the distribution of cluster and field stars. The middle and bottom panels of Fig. 4 show the corresponding Z versus $(Z-Y)$ and G versus $(G_{BP} - G_{RP})$ CMDs for clusters NGC 5617 and Trumpler 22. In Fig. 5, we used proper motion distributions of stars in the upper panels while their corresponding G , $G_{BP} - G_{RP}$ CMDs are plotted in the lower panels for clusters NGC 3293 and NGC 3324. The left panel in the

CMDs show all stars present in the cluster's area, while the middle and right panels show the probable cluster members and non-member stars respectively. By visual inspection we define the center and radius of the cluster members in VPD for a preliminary analysis. This selection was performed in a way to minimize the field star contamination and to keep the maximum possible number of lower mass stars. A circle of 0.6 mas yr^{-1} for NGC 5617, NGC 3293 and NGC 3324 while 0.4 mas yr^{-1} for Trumpler 22 around the center of the member stars distribution in the VPDs characterize our membership criteria. The picked radius is an agreement between losing cluster members with poor PMs and the involvement of non-member stars. We have also used parallax for the reliable estimation of cluster members. A star is considered as probable cluster member if it lies inside the circle in VPD and has a parallax value within 3σ from the mean cluster parallax. The CMDs of the probable members are shown in the middle and bottom row panels in each cluster CMDs as shown in Fig. 4 and Fig. 5. The main sequence of the cluster is separated. These stars have a PM error of $\leq 0.4 \text{ mas yr}^{-1}$.

For the precise estimation of mean proper motion, we deal with only probable cluster members based on clusters VPDs and CMDs as shown in Fig. 6. By fitting the Gaussian function into the constructed histograms, we determined the mean proper motion in the directions of RA and DEC, as shown in Fig. 6. From the peak of the Gaussian distribution we found mean-proper motion in RA and DEC directions for all clusters and are listed in Table 7. The estimated values of mean proper motions for each cluster are in fair agreement with the values given by Cantat-Gaudin et al. (2018). Cantat-Gaudin catalog (2018) reports the membership probabilities of few stars towards the region of clusters under study. We derived membership probabilities of each star in all the studied clusters and the adopted method has been described in the next section.

3.1 Membership Probability

Open clusters are located within the densely populated Galactic plane and contaminated by a large number of foreground/background stars. It is necessary to differentiate between cluster members and non-members, in order to derive reliable cluster fundamental parameters. In this paper, we used the membership estimation criteria for clusters NGC 5617, Trumpler 22, NGC 3293 and NGC 3324 as given by Balaguer-Núñez et al. (1998). This method has been previously used by many authors (Bellini et al. 2009, Bisht et al. 2020; Sariya et al. 2021a, 2021b; Yadav et al. 2013; Sariya & Yadav 2015). For the cluster and field star distributions, two different distribution functions (ϕ_c^v) and (ϕ_f^v) are constructed for a particular i^{th} star. The values of frequency distribution functions are given as follows:

$$\phi_c^v = \frac{1}{2\pi \sqrt{(\sigma_c^2 + \epsilon_{xi}^2)(\sigma_c^2 + \epsilon_{yi}^2)}} \times \exp\left\{-\frac{1}{2} \left[\frac{(\mu_{xi} - \mu_{xc})^2}{\sigma_c^2 + \epsilon_{xi}^2} + \frac{(\mu_{yi} - \mu_{yc})^2}{\sigma_c^2 + \epsilon_{yi}^2} \right]\right\}$$

and

$$\phi_f^v = \frac{1}{2\pi \sqrt{(1-\gamma^2)} \sqrt{(\sigma_f^2 + \epsilon_{xi}^2)(\sigma_f^2 + \epsilon_{yi}^2)}}$$

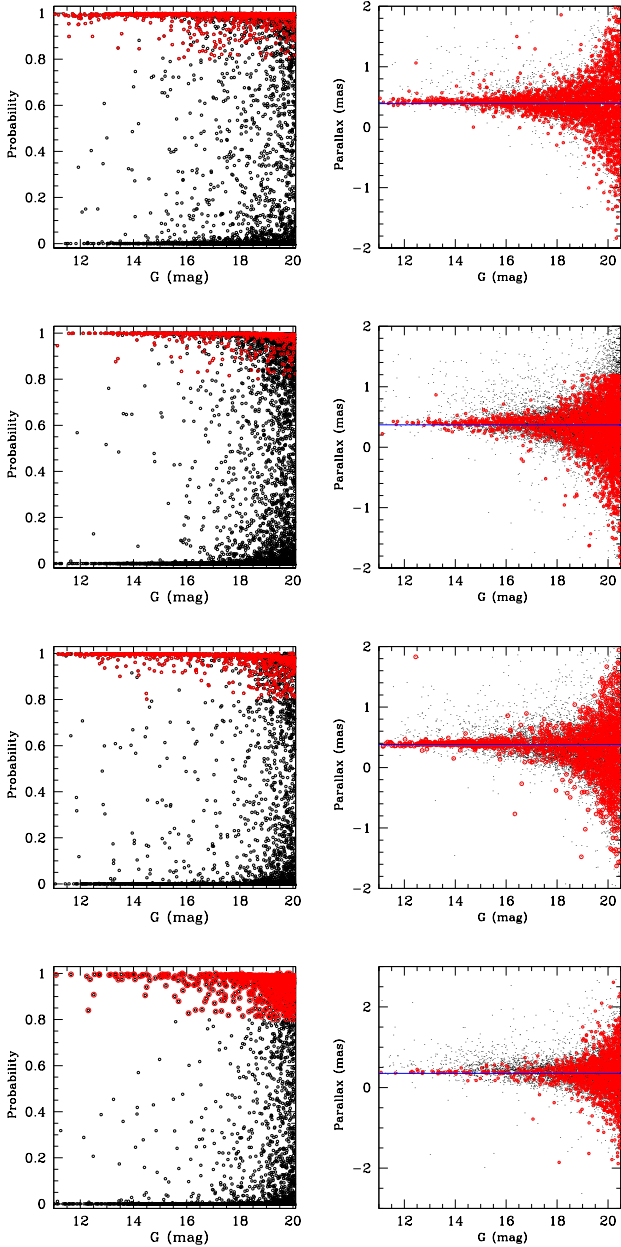


Figure 7. (Top left panel) Membership probability as a function of G magnitude for NGC 5617. (Top right panel) Parallax as a function of G magnitude for NGC 5617. Same have been plotted for clusters Trumpler 22, NGC 3293 and NGC 3324 from top to bottom. Red dots are cluster members with membership probability higher than 80%.

$$\times \exp\left\{-\frac{1}{2(1-\gamma^2)}\left[\frac{(\mu_{xi}-\mu_{xf})^2}{\sigma_{xf}^2+\epsilon_{xi}^2}-\frac{2\gamma(\mu_{xi}-\mu_{xf})(\mu_{yi}-\mu_{yf})}{\sqrt{(\sigma_{xf}^2+\epsilon_{xi}^2)(\sigma_{yf}^2+\epsilon_{yi}^2)}}+\frac{(\mu_{yi}-\mu_{yf})^2}{\sigma_{yf}^2+\epsilon_{yi}^2}\right]\right\}$$

where (μ_{xi}, μ_{yi}) are the PMs of i^{th} star. The PM errors are represented by $(\epsilon_{xi}, \epsilon_{yi})$. The cluster's PM center is given by (μ_{xc}, μ_{yc}) and (μ_{xf}, μ_{yf}) represent the center of field PM values. The intrinsic PM dispersion for the cluster stars is denoted by σ_c , whereas σ_{xf} and σ_{yf} provide

the intrinsic PM dispersion's for the field populations. The correlation coefficient γ is calculated as:

$$\gamma = \frac{(\mu_{xi}-\mu_{xf})(\mu_{yi}-\mu_{yf})}{\sigma_{xf}\sigma_{yf}}.$$

Stars with PM errors $\leq 0.5 \text{ mas yr}^{-1}$ have been used to determine ϕ_c^x and ϕ_f^y . A group of stars is found at $\mu_{xc}=-5.66 \text{ mas yr}^{-1}$, $\mu_{yc}=-3.19 \text{ mas yr}^{-1}$ for NGC 5617, $\mu_{xc}=-5.13 \text{ mas yr}^{-1}$, $\mu_{yc}=-2.70 \text{ mas yr}^{-1}$ for Trumpler 22, $\mu_{xc}=-7.65 \text{ mas yr}^{-1}$, $\mu_{yc}=3.36 \text{ mas yr}^{-1}$ for NGC 3293 and $\mu_{xc}=-7.06 \text{ mas yr}^{-1}$, $\mu_{yc}=2.85 \text{ mas yr}^{-1}$ for NGC 3324. Assuming a distance of 2.52, 2.68, 2.65 and 2.85 kpc for clusters NGC 5617, Trumpler 22, NGC 3293 and NGC 3324, respectively and radial velocity dispersion of 1 km s^{-1} for open star clusters (Girard et al. 1989), the expected dispersion (σ_c) in PMs would be $\sim 0.08 \text{ mas yr}^{-1}$ for clusters NGC 5617 and Trumpler 22 while $\sim 0.10 \text{ mas yr}^{-1}$ for other two clusters. For field region stars, we have estimated $(\mu_{xf}, \mu_{yf}) = (-3.5, -5.2) \text{ mas yr}^{-1}$ for NGC 5617, $(\mu_{xf}, \mu_{yf}) = (-3.2, -4.5) \text{ mas yr}^{-1}$ for Trumpler 22, $(\mu_{xf}, \mu_{yf}) = (-5.5, 2.0) \text{ mas yr}^{-1}$ for NGC 3293, $(\mu_{xf}, \mu_{yf}) = (-5.3, 1.3) \text{ mas yr}^{-1}$ for NGC 3324 and $(\sigma_{xf}, \sigma_{yf}) = (4.5, 4.9), (3.8, 4.1), (5.5, 4.8), (4.9, 3.7) \text{ mas yr}^{-1}$ for NGC 5617, Trumpler 22, NGC 3293 and NGC 3324, respectively.

Considering the normalized numbers of cluster stars and field stars as n_c and n_f respectively (i.e., $n_c + n_f = 1$), the total distribution function can be calculated as

$$\phi = (n_c \times \phi_c^x) + (n_f \times \phi_f^y),$$

As a result, the membership probability for the i^{th} star is given by:

$$P_\mu(i) = \frac{\phi_c(i)}{\phi(i)}.$$

In this way, we identified 584, 429, 692 and 273 stars as cluster members for NGC 5617, Trumpler 22, NGC 3293 and NGC 3324, respectively with membership probability higher than 80% and $G \leq 20 \text{ mag}$. In the top left panel and top right panel of Fig. 7, we plotted membership probability versus G magnitude and parallax versus G magnitude, respectively for cluster NGC 5617. Same have been plotted from top to bottom panels in Fig. 7 for clusters Trumpler 22, NGC 3293 and NGC 3324. For all clusters, we have plotted G versus $(G_{BP} - G_{RP})$ CMD, the identification chart and proper motion distribution using stars with membership probability higher than 80% in Fig. 8. The Cantat-Gaudin et al. (2018) catalog reports membership probabilities for all clusters under study. We matched our likely members with this catalog having membership probability higher than 80% and those have been denoted by blue dots in CMDs as shown in Fig. 14 and Fig. 15.

3.2 Determination of the effectiveness of probabilities

The stellar density of the cluster region is affected by the presence of foreground and background stars. In this regard, we have calculated the effectiveness of membership determination for the clusters under study using the

expression given below (Shao & Zhao, 1996):

$$E = 1 - \frac{N \times \sum [P_i(1-P_i)]}{\sum P_i \sum (1-P_i)}$$

where N is the total number of cluster members and P_i indicates the probability of i^{th} star of the cluster. We have found the effectiveness (E) values as 0.52, 0.55, 0.62, 0.59 for clusters NGC 5617, Trumpler 22, NGC 3293 and NGC 3324, respectively. Shao & Zhao (1996) shows that the effectiveness of membership determination of 43 open clusters ranges from 0.20 to 0.90 and the peak value is 0.55 (Wu et al. 2002). Our estimated value of effectiveness of membership determination are on the higher side for all objects.

4 ORBIT ANALYSIS OF CLUSTERS

4.1 Galactic potential model

We adopted the approach given by Allen & Santillan (1991) for Galactic potentials in clusters NGC 5617, Trumpler 22, NGC 3293 and NGC 3324. According to their model, the mass of Galaxy is described by three components: spherical central bulge, massive spherical halo, and disc. Recently Bajkova & Bobylev (2016) and Bobylev et. al (2017) refined the parameters of Galactic potential models with the help of new observational data for a distance $R \sim 0$ to 200 kpc. These potentials are given as

$$\begin{aligned} \Phi_b(r, z) &= -\frac{M_b}{\sqrt{r^2 + b_b^2}} \\ \Phi_d(r, z) &= -\frac{M_d}{\sqrt{r^2 + (a_d + \sqrt{z^2 + b_d^2})^2}} \\ \Phi_h(r, z) &= -\frac{M_h}{a_h} \ln\left(\frac{\sqrt{r^2 + a_h^2} + a_h}{r}\right) \end{aligned}$$

Where Φ_b , Φ_d and Φ_h are the potentials of central bulge, disc and halo of Galaxy respectively. r and z are the distances of objects from Galactic center and Galactic disc respectively. The halo potential is taken from Wilkinson & Evans (1999) and values of the constants are taken from Bajkova and Bobylev (2016).

4.2 Orbits Calculation

To estimate the orbits and orbital parameters for clusters under study, we have used the Galactic potential models. The input parameters, such as central coordinates (α and δ), mean proper motions ($\mu_\alpha \cos \delta$, μ_δ), parallax values, clusters age and heliocentric distances (d_\odot) for the clusters used in this paper have been taken from Table 7. The radial velocity of clusters NGC 5617 and Trumpler 22 has been taken as -38.50 ± 2.15 km/sec calculated by De Silva et al. (2015). Radial velocity of cluster NGC 3293 has been taken as -13.16 ± 0.55 km/sec from Soubiran et al. (2018) while for cluster NGC 3324, we obtained it as -14.27 ± 0.70 km/sec taking weighted mean of probable members from Gaia EDR3.

We transformed position and velocity vectors into the Galacto-centric cylindrical coordinate system using the transformation matrix given in Johnson & Soderblom (1987). In this system, (r, ϕ, z) indicates the position of an

object in Galaxy, where r is the distance from Galactic center, ϕ is the angle relative to Sun's position in the Galactic plane and z is the distance from the Galactic plane.

The right-hand coordinate system is adopted to transform equatorial velocity components into Galactic-space velocity components (U, V, W) , where U , V and W are radial, tangential, and vertical velocities respectively. In this system, the x-axis is taken positive towards Galactic-center, the y-axis is along the direction of Galactic rotation and the z-axis is towards Galactic north pole. The Galactic center is taken at $(17^h : 45^m : 32^s.224, -28^\circ : 56' : 10'')$ and North-Galactic pole is at $(12^h : 51^m : 26^s.282, 27^\circ : 7' : 42''.01)$ (Reid & Brunthaler, 2004). To apply a correction for Standard Solar Motion and Motion of the Local Standard of Rest (LSR), we used position coordinates of Sun as $(8.3, 0, 0.02)$ kpc and its space-velocity components as $(11.1, 12.24, 7.25)$ km/s (Schonrich et al. 2010). Transformed parameters in Galacto-centric coordinate system are listed in Table 1.

In orbit determination, we estimated the radial and vertical components of gravitational force, by differentiating total gravitational potentials with respect to r and z . The second order derivatives of gravitational force describe the motion of the clusters. For orbit determination, the second order derivatives are integrated backward in time, which is equal to the age of clusters. Since potentials used are axis-symmetric, energy and z component of angular momentum are conserved throughout the orbits.

Fig. 9 show orbits of the clusters NGC 5617, Trumpler 22, NGC 3293 and NGC 3324. In left panels, the motion of clusters is shown in terms of distance from the Galactic center and Galactic plane, which manifests two dimensional side view of the orbits. In middle panels, cluster motion is described in terms of x and y components of Galactocentric distance, which shows a top view of orbits. The clusters are also oscillating along Z-axis as shown in right panels of these figures. (NGC 5617 and Trumpler 22) and (NGC 3293 and NGC 3324) are oscillating along Z-axis within the limit of -0.04 to 0.04 and -0.1 to 0.1 kpc, with a time period of 67 and 79 Myr respectively. The time period of revolution around the Galactic center is 176, 172, 194 and 193 Myr for NGC 5617, Trumpler 22, NGC 3293 and NGC 3324 respectively. Time period of these oscillations for both the binary clusters are very similar. We also calculated the orbital parameters for the clusters and are listed in Table 2. Here e is eccentricity, R_a is the apogalactic distance, R_p is the perigalactic distance, Z_{max} is the maximum distance traveled by cluster from Galactic disc, E is the average energy of orbits, J_z is z component of angular momentum and T is the time period of the clusters in the orbits.

The orbits of the clusters under study follow a boxy pattern and eccentricities for all the clusters are nearly zero. Hence they trace a circular path around the Galactic center. We have shown the birth and present day position of clusters in the Galaxy which are represented by the filled circle and filled triangle respectively in Fig. 9. NGC 5617 and Trumpler 22 are intermediate age while NGC 3293 and NGC 3324 are young age OCs. The orbits are confined in a box of $\sim 6.6 < R_{gc} \leq 6.7$ kpc for (NGC 5617 and Trumpler 22) and $\sim 7.9 < R_{gc} \leq 8.6$ kpc for clusters (NGC 3293 and NGC 3324). Our analysis indicates that all the clusters under study are inside the solar circle in the thin disk and may interact with the molecular clouds present in the

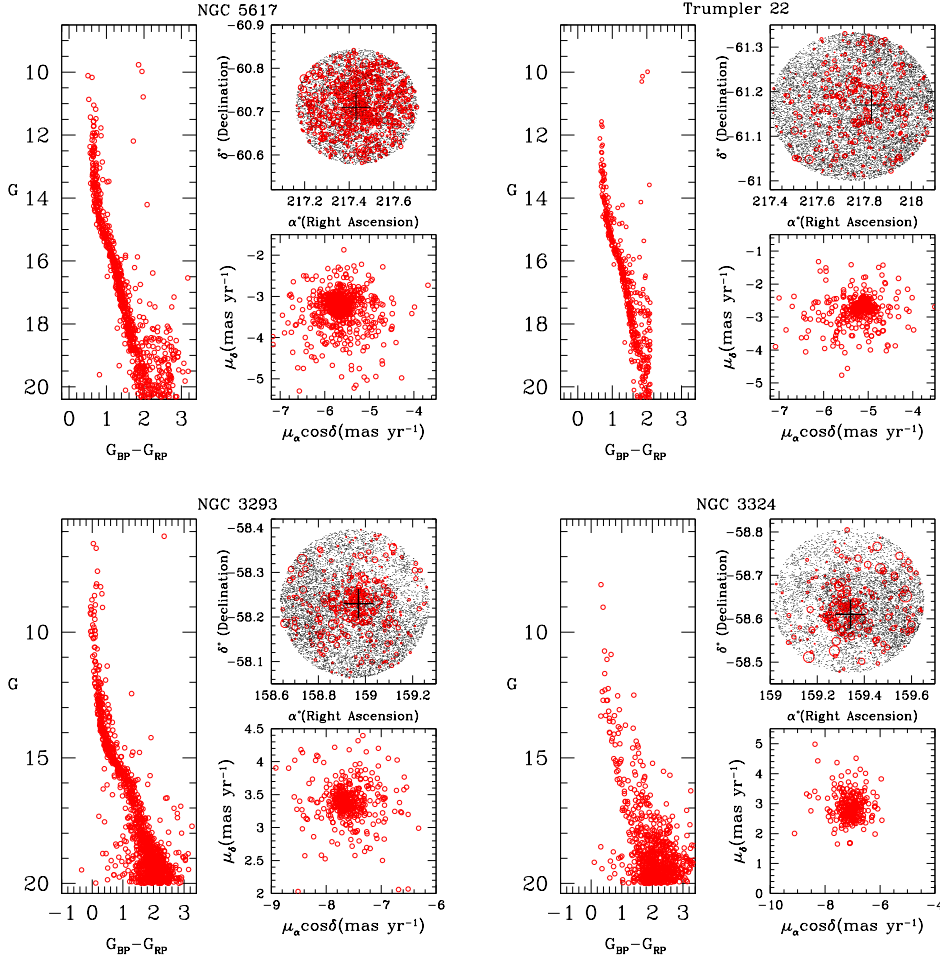


Figure 8. $(G, G_{BP} - G_{RP})$ CMDs, identification charts and proper motion distribution of member stars with membership probability higher than 80% for clusters under study. The ‘plus’ sign indicates the cluster center.

Table 1. Position and velocity components in the Galactocentric coordinate system. Here R is the galactocentric distance, Z is the vertical distance from the Galactic disc, $U V W$ are the radial tangential and the vertical components of velocity respectively and ϕ is the position angle relative to the sun’s direction.

Cluster	R (kpc)	Z (kpc)	U (km/s)	V (km/s)	W (km/s)	ϕ (radian)
NGC 5617	6.81	0.02	-7.80 ± 1.62	-241.30 ± 1.63	2.61 ± 1.54	0.26
Trumpler 22	6.71	-0.01	0.46 ± 1.66	-242.41 ± 1.66	-0.49 ± 1.25	0.28
NGC 3293	7.99	0.02	-10.98 ± 0.37	-257.23 ± 0.55	3.54 ± 0.56	0.32
NGC 3324	7.98	0.01	-2.45 ± 8.42	-257.82 ± 4.32	5.76 ± 2.53	0.34

Table 2. Orbital parameters for the clusters obtained using the Galactic potential model.

Cluster	e	R_a (kpc)	R_p (kpc)	Z_{max} (kpc)	E (100km/s) ²	J_z (100 kpc km/s)	T (Myr)
NGC 5617	0.01	6.75	6.66	0.03	-12.33	-16.44	176
Trumpler 22	0.003	6.70	6.66	0.01	-12.40	-16.27	172
NGC 3293	0.04	8.54	7.90	0.05	-10.95	-20.56	194
NGC 3324	0.04	8.62	8.03	0.08	-10.94	-20.58	193

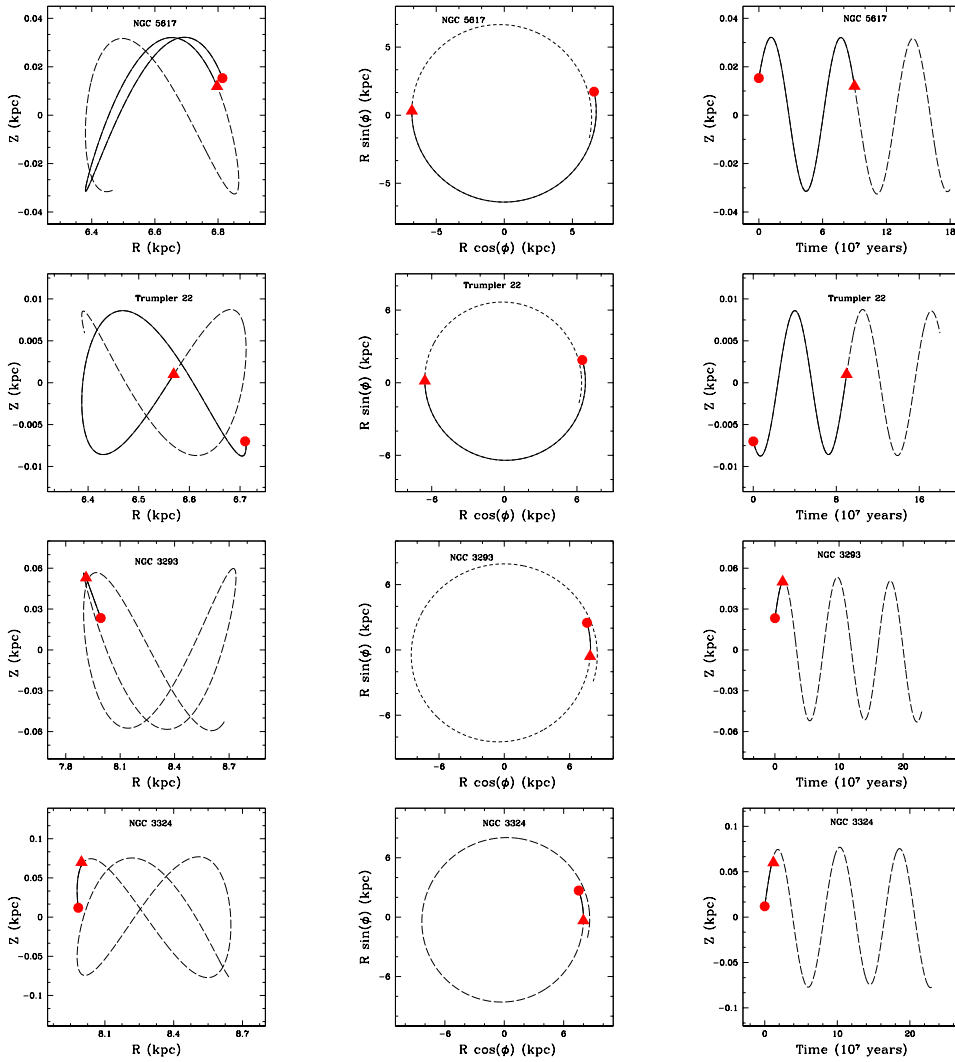


Figure 9. Galactic orbits of the clusters NGC 5617, Trumpler 22, NGC 3293 and NGC 3324 estimated with the Galactic potential model described in the text, in the time interval of the age of each cluster. The left panel shows a side view, the middle panel shows a top view and the right panel shows period of oscillation along Z-axis of the cluster’s orbit. The continuous and dotted lines in this figure are for 90 Myr (age) and 180 Myr for cluster pair NGC 5617 and Trumpler 22 while 12 Myr (age) and 230 Myr for cluster pair NGC 3293 and NGC 3324, respectively. The curves with dotted lines represent the complete cycle. The filled triangle and filled circle denotes birth and present day position of clusters in the Galaxy.

Galaxy. Carraro & Chiosi (1994) found that clusters orbiting beyond the solar circle survive more as compared to the clusters which are in the inner solar circle. Webb et al. (2014) found that clusters having circular orbits evolve slower as compared to the eccentric ones. Orbital parameters determined in the present analysis are very much similar to the parameters found by Wu et al. (2009), except their orbits, are more eccentric than what we found in the present analysis.

5 STRUCTURAL PARAMETERS OF THE CLUSTERS

5.1 Cluster center

The central coordinates of OCs play an important role to describe cluster properties more accurately. In the previous studies, the center has been determined just by the visual inspection (Becker & Fenkart 1971; Romanishim & Angel 1980). We applied the star-count method using probable cluster members based on proper motion and parallax database. The histograms are built for clusters NGC 5617, Trumpler 22, NGC 3293 and NGC 3324 in both the RA and DEC directions as shown in Fig. 10. The Gaussian curve-fitting is performed to the star counts profiles in RA and DEC directions. All estimated center coordinates are listed in Table 7. Our estimated values are in good agreement with

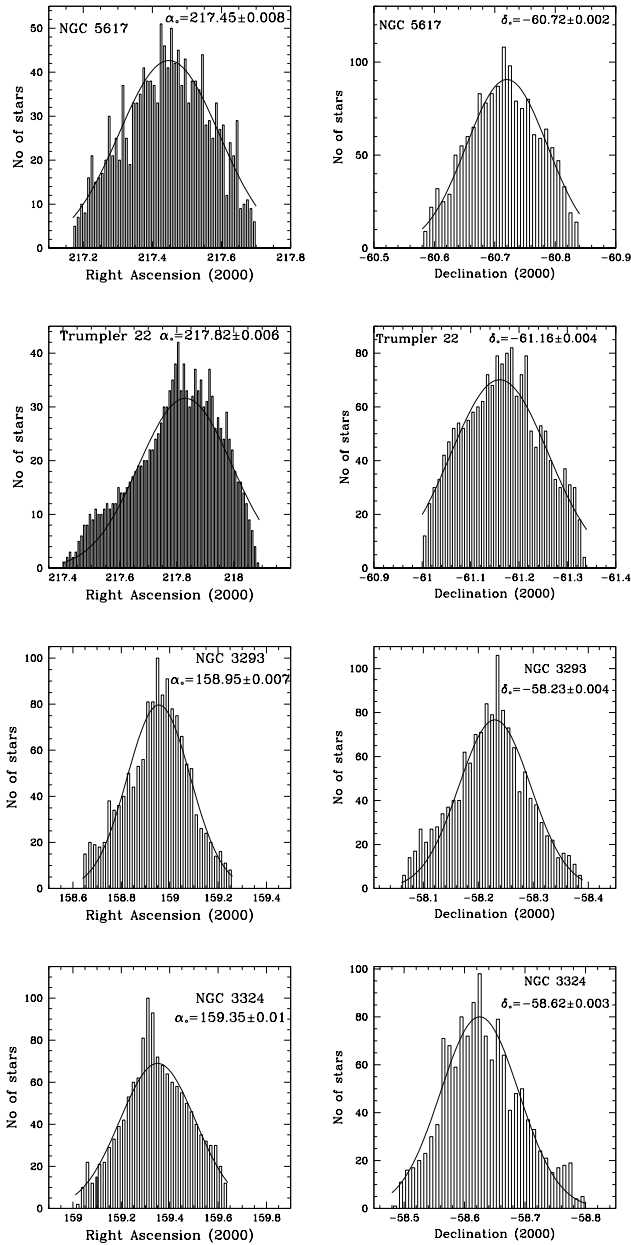


Figure 10. Profiles of stellar counts across clusters NGC 5617, Trumpler 22, NGC 3293 and NGC 3324 using Gaia EDR3. The Gaussian fits have been applied. The center of symmetry about the peaks of Right Ascension and Declination is taken to be the position of the cluster's center.

the values given by Dias et al. (2002). Our derived center coordinates for all objects are also coordinated with Cantat-Gaudin et al. (2018) catalog within uncertainty.

5.2 Radial density profile

To estimate the structural parameters of the cluster, we have plotted the radial density profile (RDP) for OCs NGC 5617, Trumpler 22, NGC 3293 and NGC 3324. We have organized clusters area in many concentric circles

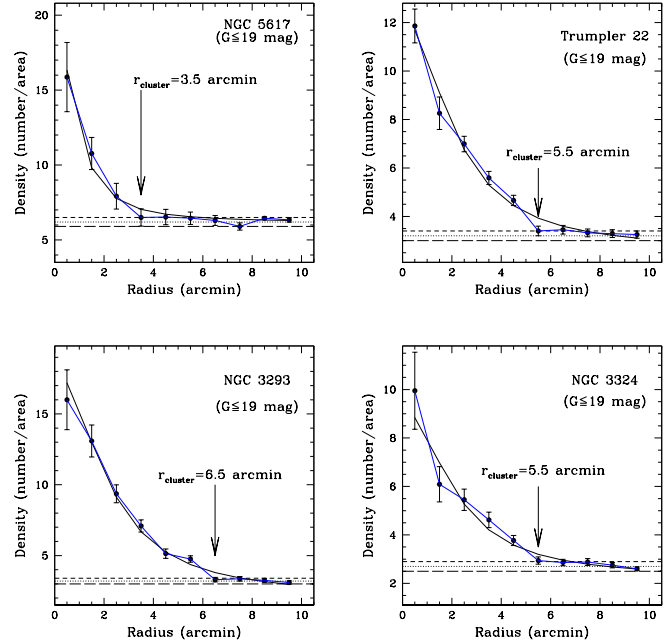


Figure 11. Surface density distribution of the clusters under study. Errors are determined from sampling statistics ($= \frac{1}{\sqrt{N}}$ where N is the number of stars used in the density estimation at that point). The smooth line represent the fitted profile whereas dotted line shows the background density level. Long and short dash lines represent the errors in background density.

around the cluster's core having equal incremental radii. The number density, ρ_i , in the i^{th} zone is calculated by adopting the formula, $\rho_i = \frac{N_i}{A_i}$, where N_i is the number of cluster members and A_i is the area of the i^{th} zone. Based on the visual inspection in clusters RDPs, the distance at which each distribution flattens is considered as cluster radius. The error in the background density level is shown with dotted lines in Fig. 11. RDP becomes flat at $r \sim 3.5'$, $5.5'$, $6.5'$ and $5.5'$ for the clusters NGC 5617, Trumpler 22, NGC 3293 and NGC 3324, respectively. After this distance from the cluster center, cluster stars merged with field stars as clearly shown in Fig. 11. Accordingly, we considered $3.5'$, $5.5'$, $6.5'$ and $5.5'$ as the cluster radius for clusters under study. The observed radial density profile was fitted using King (1962) profile:

$$f(r) = f_b + \frac{f_0}{1+(r/r_c)^2}$$

where r_c , f_0 , and f_{bg} are the core radius, central density, and the background density level, respectively. By fitting the King model to RDPs, we have derived the structural parameters for clusters NGC 5617, Trumpler 22, NGC 3293 and NGC 3324.

Limiting radius (r_{lim}) of each cluster is calculated by comparing $f(r)$ to a background density level, f_b , defined as

$$f_b = f_{bg} + 3\sigma_{bg}$$

Table 3. Structural parameters of the clusters under study. Background and central density are in the unit of stars per arcmin². Core radius (r_c) and tidal radius (R_t) are in arcmin and pc.

Name	f_0	f_b	r_c arcmin	r_c parsec	δ_c	r_{lim} arcmin	c
NGC 5617	19.28	6.20	0.93	0.66	4.1	3.6	0.58
Trumpler 22	12.17	3.20	2.2	1.7	4.8	6.6	0.47
NGC 3293	17.96	3.20	2.5	1.9	6.5	9.3	0.57
NGC 3324	9.18	2.70	1.8	1.5	4.4	4.6	0.41

where σ_{bg} is uncertainty of f_{bg} . Therefore, r_{lim} is calculated according to the following formula (Bukowiecki et al. 2011)

$$r_{lim} = r_c \sqrt{\left(\frac{f_0}{3\sigma_{bg}} - 1\right)}$$

Maciejewski & Niedzielski (2007) suggested that r_{lim} may vary for particular clusters from $2r_c$ to $7r_c$. In present study, all clusters show a good agreement with Maciejewski & Niedzielski (2007).

The density contrast parameter ($\delta_c = 1 + \frac{f_0}{f_b}$) is calculated for all the clusters under study using member stars selected from proper motion data. Current evaluation of δ_c (4.1, 4.8, 6.5 and 4.4 for NGC 5617, Trumpler 22, NGC 3293 and NGC 3324, respectively) are lower than the values ($7 \leq \delta_c \leq 23$) given by Bonatto & Bica (2009). This estimation of δ_c indicates that all clusters are sparse.

6 THE FUNDAMENTAL PARAMETERS OF NGC 5617 AND TRUMPLER 22

6.1 Two colour diagrams

The two-colour diagrams (TCDs) are very useful to determine the relation of various colour-excesses and their variations towards the cluster region.

6.1.1 Optical to mid-infrared extinction law

In this section, we combined multi-wavelength photometric data with Gaia astrometry for clusters under study to check the extinction law from optical to mid-infrared region. The resultant $(\lambda - G_{RP}) / (G_{BP} - G_{RP})$ two colour diagrams (TCDs) are shown in Fig. 12 for all the clusters. Here, λ denotes the filters other than G_{RP} . All stars showing in Fig. 12 are probable cluster members. A linear fit to the data points is performed and slopes are listed in Table 4. The estimated values of slopes are in good agreement with the value given by Wang & Chen (2019) only for binary clusters NGC 5617 and Trumpler 22. We estimated $R = \frac{A_V}{E(B-V)}$ as ~ 3.1 for clusters NGC 5617 and Trumpler 22. Our obtained values of R are ~ 3.8 and 1.9 for clusters NGC 3293 and NGC 3324. Our analysis indicates that reddening law is normal towards the cluster region of NGC 5617 and Trumpler 22 while it is abnormal for binary clusters NGC 3293 and NGC 3324.

6.1.2 Interstellar reddening from JHK colours

To estimate the cluster reddening in the near-IR region, we used $(J - H)$ versus $(J - K)$ colour-colour diagrams as shown in Fig. 13. Stars plotted in this figure are the probable cluster members described in Sec. 3. The solid line is the cluster's zero age main sequence (ZAMS) taken from Caldwell et al. (1993). The ZAMS shown by the dotted line is displaced by the value of $E(J - H)$ and $E(J - K)$ for all clusters are given in Table 7. In this figure, the solid line is theoretical isochrone taken from Marigo et al. (2017) of $\log(\text{age})=8.25$ and 7.05 for binary clusters (NGC 5617 and Trumpler 22) and (NGC 3293 and NGC 3324), respectively. The ratio of $E(J - H)$ and $E(J - K)$ shows a good agreement with the normal value 0.55 proposed by Cardelli et al. (1989). We have estimated the interstellar reddening, $E(B - V)$ using the following relations (Fiorucci & Munari, 2003):

$$E(J - H) = 0.309 \times E(B - V)$$

$$E(J - K) = 0.48 \times E(B - V)$$

Using the above relationships, we obtained the interstellar reddening, $E(B - V)$ as, 0.55, 0.64, 0.23 and 0.45 for the clusters NGC 5617, Trumpler 22, NGC 3293 and NGC 3324, respectively. Our derived value of $E(B - V)$ is similar to Haug (1978) and slightly higher than KF91 for NGC 5617. Our $E(B - V)$ value for NGC 3324 is in good agreement with the value obtained by Claria (1977).

6.2 Age and distance to the clusters

To trace the Galactic structure and chemical evolution of the Galaxy using OCs, the distance, and age of OCs play the most important role (Friel & Janes 1993). We have estimated the mean value of A_G for the studied clusters using the most probable members from Gaia DR2. Our values are 1.58, 1.65, 0.86 and 0.75 for clusters NGC 5617, Trumpler 22, NGC 3293 and NGC 3324, respectively. The main fundamental parameters (age, distance, and reddening) are estimated by fitting the solar metallicity ($Z = 0.019$) isochrones of Marigo et al. (2017) to all the CMDs $(G, G_{BP} - G_{RP})$, $(G, G_{BP} - G)$, $(G, G - G_{RP})$, $(Z, Z - Y)$, $(J, J - H)$ & $(K, J - K)$ as shown in Fig. 14 and Fig. 15. We have used only probable cluster members in order to reduce the field star contamination in the cluster's area.

The galactocentric coordinates of the clusters X (directed towards the galactic center in the Galactic disc), Y

Table 4. Multi-band colour excess ratios in the direction of clusters NGC 5617, Trumpler 22, NGC 3293 and NGC 3324.

Band (λ)	Effective wavelength (nm)	NGC 5617	$\frac{\lambda - G_{RP}}{G_{BP} - G_{RP}}$ Trumpler 22	NGC 3293	NGC 3324
Johnson B	445	1.60 ± 0.03	1.61 ± 0.02	1.27 ± 0.03	1.33 ± 0.01
Johnson V	551	0.88 ± 0.02	0.94 ± 0.01	0.65 ± 0.02	0.50 ± 0.02
VPHAS i	725	0.13 ± 0.02	0.12 ± 0.04	0.04 ± 0.03	0.04 ± 0.04
VPHAS r	620	0.68 ± 0.04	0.66 ± 0.05	0.44 ± 0.05	0.44 ± 0.05
VPHAS h_α	659	0.63 ± 0.06	0.68 ± 0.07	0.24 ± 0.07	0.30 ± 0.04
VPHAS g	485	1.49 ± 0.09	1.52 ± 0.08	1.15 ± 0.08	1.33 ± 0.12
VPHAS u	380	2.60 ± 0.10	2.59 ± 0.11	2.10 ± 0.11	2.17 ± 0.10
J	1234.5	-0.77 ± 0.03	-0.80 ± 0.05	-0.90 ± 0.04	-1.07 ± 0.07
H	1639.3	-1.20 ± 0.05	-1.24 ± 0.05	-1.07 ± 0.05	-1.09 ± 0.06
K	2175.7	-1.33 ± 0.06	-1.39 ± 0.07	-1.20 ± 0.09	-1.31 ± 0.09
WISE W1	3317.2	-1.37 ± 0.09	-1.40 ± 0.08	-1.22 ± 0.10	-1.21 ± 0.08
WISE W2	4550.1	-1.43 ± 0.10	-1.42 ± 0.09	-1.17 ± 0.12	-1.15 ± 0.11

(directed towards the Galactic rotation) and distance from the galactic plane Z (directed towards Galactic north pole) can be estimated using clusters' distances, longitude, and latitude. The Galactocentric distance has been calculated by considering 8.5 kpc as the distance of the Sun to the Galactic center. The estimated Galactocentric coordinates are listed in Table 7.

The estimation of the main fundamental parameters for the clusters are given below:

NGC 5617: We fitted the theoretical isochrones of different ages ($\log(\text{age})=7.90, 7.95$ and 8.00) in all the CMDs for the cluster NGC 5617, shown in the upper panels of Fig. 14. The best global fit is favorable for the middle isochrone with $\log(\text{age})=7.95$ to the high mass cluster members. A satisfactory fitting of isochrones provides an age of 90 ± 10 Myr. The apparent distance modulus ($m - M = 13.70 \pm 0.4$ mag) provides a distance 2.5 ± 0.30 kpc from the Sun. The estimated distance is in good agreement with the value of 3.0 kpc as given by Cantat-Gaudin et al. (2018).

Trumpler 22: In the CMDs of Trumpler 22, we have fitted exactly the similar age isochrones as shown in Fig. 14. So, the age of this object is the same as that of NGC 5617. The inferred apparent distance modulus ($m - M = 14.20 \pm 0.3$ mag) provides a heliocentric distance as 2.8 ± 0.2 kpc. This value of the distance is very close to the distance derived by Cantat-Gaudin et al. (2018).

NGC 3293: For cluster NGC 3293, we have fitted the theoretical isochrones of different ages ($\log(\text{age})=7.00, 7.05$ and 7.10) as shown in Fig. 15. Based on the best fitted middle isochrone of $\log(\text{age})=7.05$, we found the age of this object as 12 ± 2 Myr. The inferred apparent distance modulus ($m - M = 12.90 \pm 0.2$ mag) provides a heliocentric distance as 2.6 ± 0.1 kpc. This value of the distance is very close to the distance derived by Cantat-Gaudin et al. (2018).

NGC 3324: For this cluster also, the isochrones of the same age values as NGC 3293 were fitted (see Fig. 15). The inferred apparent distance modulus ($m - M = 13.00 \pm 0.2$) mag provides a heliocentric distance of 2.8 ± 0.2 kpc. This value of the distance is very close to the distance derived by Cantat-Gaudin et al. (2018).

We have used kinematical data from Gaia EDR3 to esti-

mate the distances of clusters NGC 5617, Trumpler 22, NGC 3293 and NGC 3324. We can estimate cluster distance using the mean parallax of probable members (Lauri et al. 2018). The Gaia DR2 parallax has been corrected for these clusters after adopting zero-point offset (-0.05 mas) as given by Riess et al. (2018). The histograms of parallax using probable members in all clusters with 0.15 mas bins are shown in Fig. 16. The mean parallax is estimated as 0.41 ± 0.008 mas, 0.38 ± 0.009 mas, 0.39 ± 0.004 mas and 0.36 ± 0.01 mas for the clusters NGC 5617, Trumpler 22, NGC 3293 and NGC 3324, respectively and the corresponding distance values are 2.44 ± 0.05 kpc, 2.63 ± 0.06 kpc, 2.56 ± 0.02 kpc and 2.77 ± 0.07 kpc. These obtained values of distance are reciprocal of cluster parallax. The mean parallax for all clusters are very close to the parallax obtained by Cantat-Gaudin et al. (2018). We also determined the distance of the clusters according to the method discussed by Bailer-Jones et al. (2018). In this way, our estimated values are 2.43 ± 0.08 kpc, 2.64 ± 0.07 kpc, 2.59 ± 0.1 kpc and 2.80 ± 0.2 kpc for clusters NGC 5617, Trumpler 22, NGC 3293 and NGC 3324, respectively. The estimated values of cluster distance are also in good agreement with the results obtained using the isochrone fitting method as described in the above paragraph.

6.3 Young stellar object candidates

A star can be considered a young stellar object candidate (YSO) if the free reddening parameter (Q) becomes less than -0.05 mag (Buckner & Froebrich (2013)). This Q value can be estimated for stars using the relationship given by Buckner & Froebrich (2013) as below,

$$Q = (J - H) - 1.55 \times (H - K),$$

Here J , H , and K are the VVV photometric magnitudes of stars. Using the above relation, we obtained a total of 18 and 44 members as YSOs towards the cluster region of NGC 5617 and Trumpler 22, respectively. These identified YSOs have been plotted in Fig. 17 with blue dots in each panel.

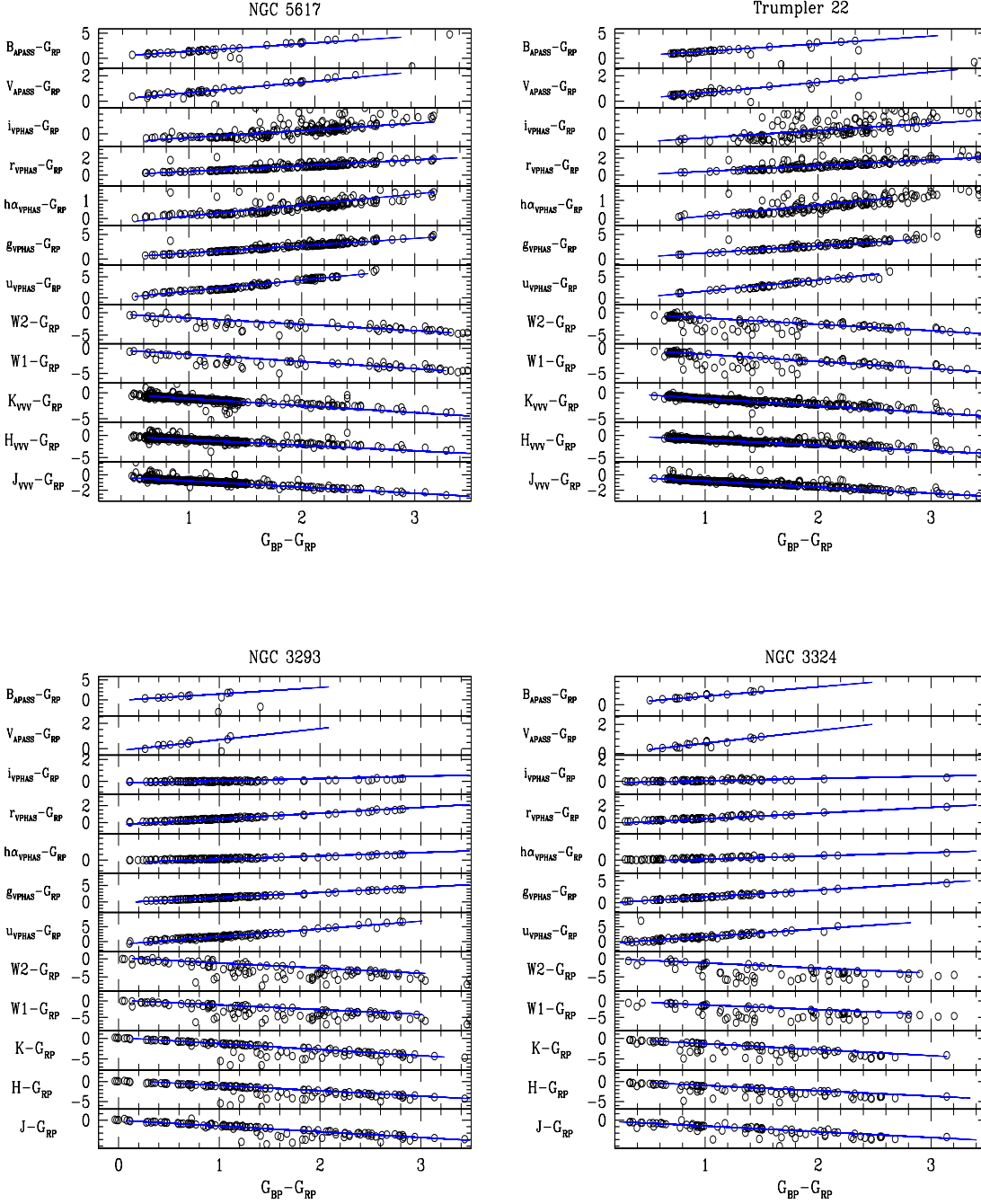


Figure 12. The $(\lambda - G_{RP})/(G_{BP} - G_{RP})$ TCDs using the stars selected from VPDs of clusters NGC 5617, Trumpler 22, NGC 3293 and NGC 3324. The continuous lines represent the slope determined through least-squares linear fit.

7 DYNAMICAL STUDY OF THE CLUSTERS

7.1 Luminosity function and Mass function

Luminosity function (LF) and Mass function (MF) are primarily dependent on cluster membership and also connected with the well known mass-luminosity relationship. To construct the LF for clusters NGC 5617, Trumpler 22, NGC

3293 and NGC 3324 we used G versus $(G_{BP} - G_{RP})$ CMD. We converted the G magnitudes of main sequence stars into the absolute magnitudes using the distance modulus and reddening calculated in this paper for all clusters. A histogram is constructed with 1.0 mag intervals as shown in Fig. 18. This figure exhibits that the LF continues to increase up to $M_G \sim 3.4, 2.0, 3.3$ and 5.2 mag for clusters

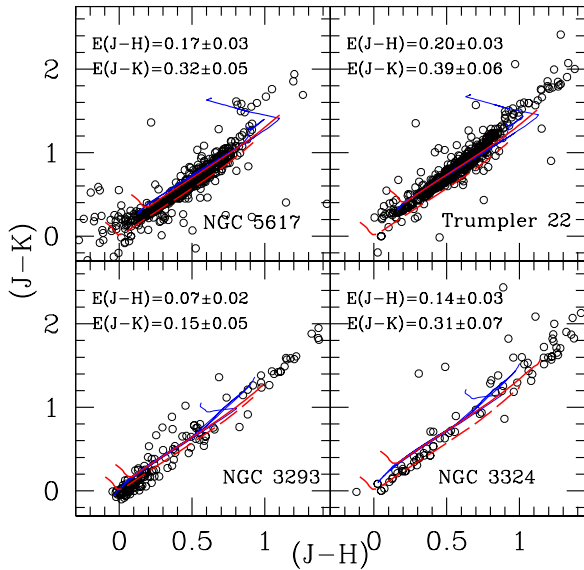


Figure 13. The colour-colour diagrams (CCDs) for clusters under study using probable cluster members. In CCDs, the red solid line is the ZAMS taken from Caldwell et al. (1993) while the red dotted lines are the same ZAMS shifted by the values as described in the text. The blue line is the theoretical isochrones of $\log(\text{age})=7.95$ and 7.05 for cluster pair (NGC 5617 and Trumpler 22) and (NGC 3293 and NGC 3324), respectively.

NGC 5617, Trumpler 22, NGC 3293 and NGC 3324, respectively.

We have used the theoretical isochrones of Marigo et al. (2017) to convert the LF into MF. To understand the MF, we have converted absolute mag bins to mass bins and the resulting mass function is shown in Fig. 19. The MF slope can be acquired by using a power-law given by,

$$\log \frac{dN}{dM} = -(1+x) \log(M) + \text{constant}$$

Where dN is the probable cluster members in a mass bin dM with central mass M and x is mass function slope. Since Gaia data (G mag) is not complete below $G=19$ mag (Arenou et al. 2018) then we took stars brighter than this limit, which corresponds to stars more massive than $1 M_{\odot}$. The estimated values of the MF slopes are $x = 1.40 \pm 0.16$, 1.44 ± 0.24 , 1.59 ± 0.22 and 1.51 ± 0.25 for clusters NGC 5617, Trumpler 22, NGC 3293 and NGC 3324, respectively. These obtained values are satisfactory with the Salpeter's initial mass function slope within error. The Total mass has been estimated for clusters using the derived mass function slope. All MF related parameters in this section, like mass range, mass function slope, and the total mass estimated are listed in Table 5.

7.2 Mass-segregation

In mass segregation, the higher mass stars gradually sink towards the cluster center and transfer their kinetic energy to the more numerous lower-mass stellar component. Mass-

Table 5. The main mass function parameters in clusters.

Object	Mass range M_{\odot}	MF slope	Total mass M_{\odot}	Mean mass M_{\odot}
NGC 5617	1.3 – 4.0	1.40 ± 0.16	1230	2.10
Trumpler 22	1.0 – 4.1	1.44 ± 0.24	755	1.76
NGC 3293	1.1 – 6.8	1.59 ± 0.22	1457	2.10
NGC 3324	1.1 – 6.8	1.51 ± 0.25	580	2.12

Table 6. Distribution of stars in different mass ranges along with the percentage of confidence level in mass-segregation effect for the clusters.

Object	Mass range M_{\odot}	Confidence level %
NGC 5617	4.0 – 2.4, 2.4 – 1.2, 1.2 – 0.8	88
Trumpler 22	4.1 – 2.6, 2.6 – 1.3, 1.3 – 0.8	75
NGC 3293	6.9 – 2.2, 2.2 – 1.2, 1.2 – 0.8	77
NGC 3324	6.9 – 2.1, 2.1 – 1.2, 1.2 – 0.8	70

segregation effect in clusters can be due to the dynamical evolution or imprint of the star formation process or both. Considerable work has been done by many authors to check the mass segregation effect in clusters (Hillenbrand & Hartmann 1998; Lada & Lada 1991; Brandl et al. 1996; Meylan 2000, Bisht et al. 2019, 2020). In this study, we used only probable cluster members based on membership probability as described in section 3. To understand mass-segregation cluster stars are divided into three different mass-ranges as shown in Table 6 for clusters NGC 5617, Trumpler 22, NGC 3293 and NGC 3324. The cumulative radial stellar distribution has been plotted for the main sequence stars of all objects as shown in Fig. 20. This figure demonstrates the mass segregation effect in these clusters based on the arrangement of massive and faint stars. We found the confidence level of mass-segregation as 88 %, 75 %, 77 % and 70 % for the clusters NGC 5617, Trumpler 22, NGC 3293 and NGC 3324, respectively based on Kolmogorov-Smirnov test.

In the lifetime of star clusters, encounters between its member stars gradually lead to an increased degree of energy equipartition throughout the clusters. The time scale on which a cluster will lose all traces of its initial conditions is well represented by its relaxation time T_R , which is given by

$$T_R = \frac{8.9 \times 10^5 \sqrt{N} \times R_h^{3/2}}{\sqrt{m} \times \log(0.4N)}$$

In the above formula, N denotes the cluster members, R_h is the radius within which half of the cluster mass is accommodated and m is the mean mass of the cluster stars (Spitzer & Hart 1971).

The value of R_h can be estimated based on the transformation equation given in Larsen (2006),

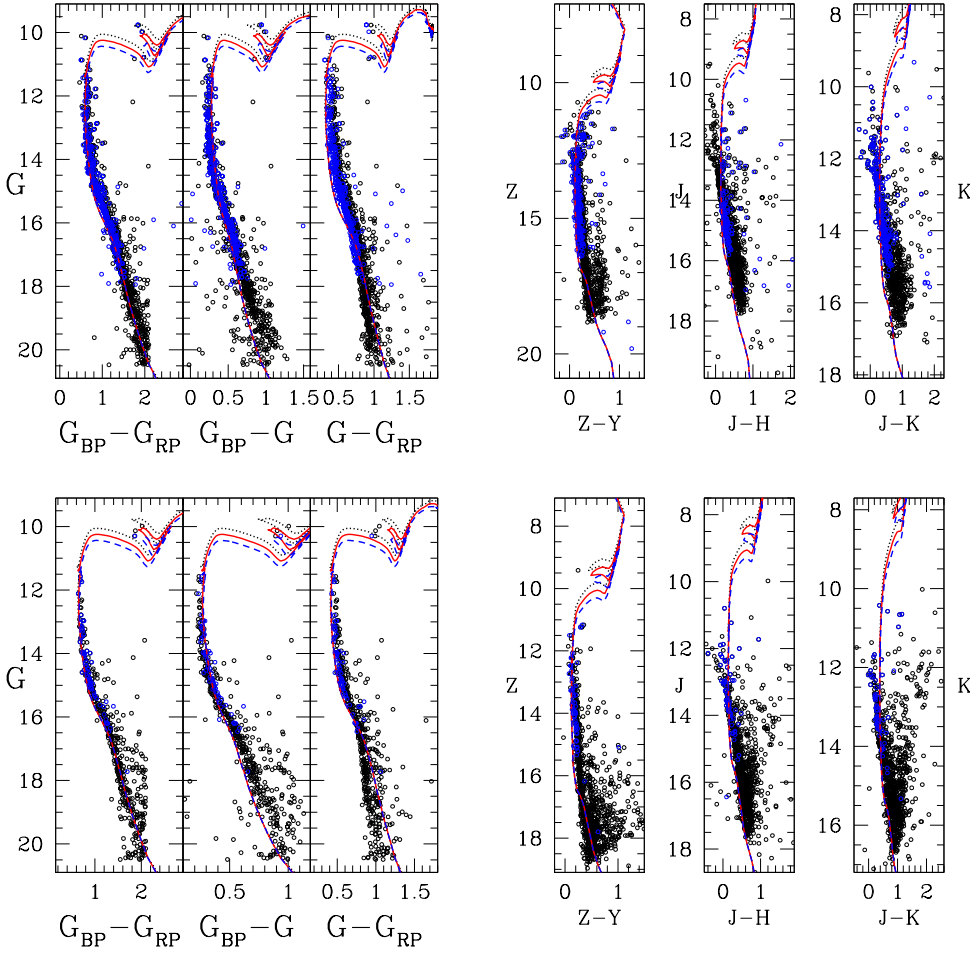


Figure 14. The G , $(G_{BP} - G_{RP})$, G , $(G_{BP} - G)$, G , $(G - G_{RP})$, Z , $(Z - Y)$, J , $(J - H)$ and K , $(J - K)$ colour-magnitude diagrams of open star cluster NGC 5617 (top panels) and Trumpler 22 (bottom panels). Black open circles show the most probable cluster members as selected from VPDs. The curves represent the isochrones of $(\log(\text{age})=7.90, 7.95 \text{ and } 8.00)$ for both clusters. All these isochrones are taken from Marigo et al. (2017) for solar metallicity. Blue dots are the matched stars with Cantat-Gaudin (2018) having membership probability higher than 80%.

$$R_h = 0.547 \times R_c \times \left(\frac{R_t}{R_c}\right)^{0.486}$$

where R_c is core radius while R_t is tidal radius. We obtained the value of half light radius as 1.67, 2.50, 2.52 and 2.28 pc for clusters NGC 5617, Trumpler 22, NGC 3293 and NGC 3324, respectively.

We estimated the value of T_R as 13.5, 24.5, 26 and 17 Myr for NGC 5617, Trumpler 22, NGC 3293 and NGC 3324, respectively. The dynamical evolution parameter ($\tau = \frac{a q c}{T_E}$) are found to be greater than 1 for clusters NGC 5617 and Trumpler 22, which concludes that these objects are dynamically relaxed. The value of τ is less than 1 for clusters NGC 3293 and NGC 3324. Hence our study demonstrates that the binary clusters NGC 3293 and NGC 3324 are not dynamically relaxed.

7.3 Dissociation time of clusters

The compact N-body stellar groups have to be eventually demolished tidally, either by the Galactic field or by the nearby transit of any giant molecular clouds (Converse & Stahler 2011). We have estimated the dissociation time of both clusters using the relationship given by Binney & Tremaine (2008)

$$t_{dis} = 250 \left(\frac{M}{300}\right)^{1/2} \times \left(\frac{R_h}{2}\right)^{-3/2}$$

M and R_h are the total cluster mass and half mass radius of the clusters. We have estimated dissociation time as 664, 282, 390 and 285 Myr for clusters NGC 5617, Trumpler 22, NGC 3293 and NGC 3324, respectively. These estimated values of dissociation time for all objects are very high than their relaxation times. These obtained values of dissociation time indicate that NGC 5617, Trumpler 22, NGC 3293 and NGC 3324 should turn apart after the death of their bright members throughout the quick expansion of these objects.

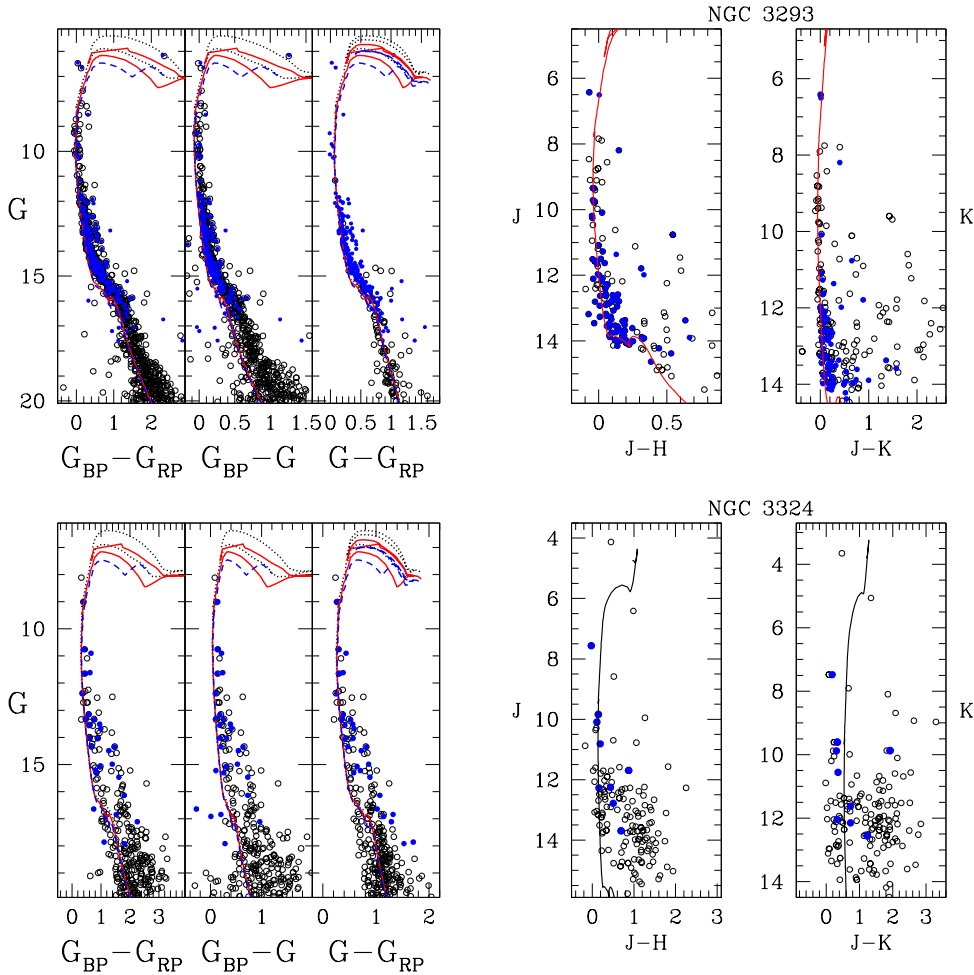


Figure 15. The G , $(G_{BP} - G_{RP})$, G , $(G_{BP} - G)$, G , $(G - G_{RP})$, J , $(J - H)$ and K , $(J - K)$ colour-magnitude diagrams of open star cluster NGC 3293 (top panels) and NGC 3324 (bottom panels). Black open circles are probable cluster members as selected from VPDs. The curves are the isochrones of $(\log(\text{age})=7.00, 7.05 \text{ and } 7.10)$ in the CMDs of the Gaia Bands. We used the middle age isochrone of $\log(\text{age})=7.05$ in J , $(J - H)$ and K , $(J - K)$ CMDs. All these isochrones are taken from Marigo et al. (2017) for solar metallicity. Blue dots are the matched stars with Cantat-Gaudin (2018) having membership probability higher than 80%.

7.4 Tidal Radius of the clusters

Tidal interactions are crucial to understand the initial structure and dynamical evolution of the clusters (Chumak et al. 2010). Tidal radius is the distance from the cluster center where gravitational acceleration caused by the cluster becomes equal to the tidal acceleration due to parent Galaxy (von Hoerner 1957). The Galactic mass M_G inside a Galactocentric radius R_G is given by (Genzel & Townes, 1987),

$$M_G = 2 \times 10^8 M_\odot \left(\frac{R_G}{30 \text{ pc}} \right)^{1.2}$$

Estimated values of Galactic mass inside the Galactocentric radius (see Sec. 4.5) are found as $2.4 \times 10^{11} M_\odot$ and $1.6 \times 10^{11} M_\odot$ for cluster pairs (NGC 5617 and Trumpler 22) and (NGC 3293 and NGC 3324), respectively. Kim et al. (2000) has introduced the formula for tidal radius R_t of clusters as,

$$R_t = \left(\frac{M}{2M_G} \right)^{1/3} \times R_G$$

where R_t and M are the tidal radius and the total mass of the clusters. The estimated values of the tidal radius are 15.06, 12.94, 13.36 and 9.98 pc for NGC 5617, Trumpler 22, NGC 3292 and NGC 3324, respectively.

8 BINARITY OF THE CLUSTERS

Using the photometry and high resolution spectroscopy, de Silva et al. (2018) studied the physical connection between NGC 5617 and Trumpler 22. Based on the age and chemical composition they concluded that these clusters are a primordial binary cluster pair in the Milky Way. To check the physical connection we estimated the separation between these two binary clusters using the relation given by de la Fuente Marcos & de la Fuente Marcos (2010),

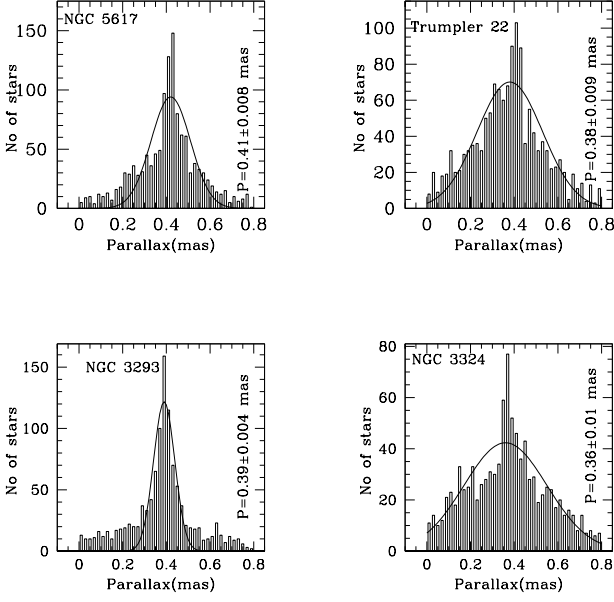


Figure 16. Histogram for parallax estimation of the clusters NGC 5617, Trumpler 22, NGC 3293 and NGC 3324 using probable cluster members based on clusters VPDs. The Gaussian function is fitted to the central bins provides a mean value of parallax. The dashed line is the mean value of clusters parallax.

$$P_{orb}(Myr) = 94 \left(\frac{S_0}{1+e_0} \right)^{3/2} \times \frac{1}{\sqrt{M_1+M_2}}$$

where P_{orb} is orbital time period, e_0 is eccentricity, M_1 and M_2 are the total masses of clusters and S_0 is the separation between the binary clusters. Using the above relation, we obtained the separation as ~ 18 pc and ~ 19 pc for clusters pairs (NGC 5617 and Trumpler 22) and (NGC 3293 and NGC 3324). The small value of separation indicates that these objects are bound.

We analyzed the orbits of both the cluster pairs. All clusters are orbiting in a circular orbit. Their close values of orbital parameters indicate that they are moving together. Their distance and age also indicate that they have formed in a similar time scale. Therefore, based on the motion we can conclude that these clusters are a cluster pairs of our Galaxy.

9 CONCLUSIONS

One of the outcomes of this study is the estimation of membership probability of stars in the field of the two binary clusters (NGC 5617 and Trumpler 22) and (NGC 3293 and NGC 3324). We have estimated all the fundamental parameters of the clusters as shown in Table 7. The main conclusions of the present study are as follows:

- (i) The new center coordinates are derived for all clusters and are listed in Table 7.
- (ii) Colour-colour diagrams have been constructed after combining Gaia EDR3, VVV, VPHAS, APASS, and WISE

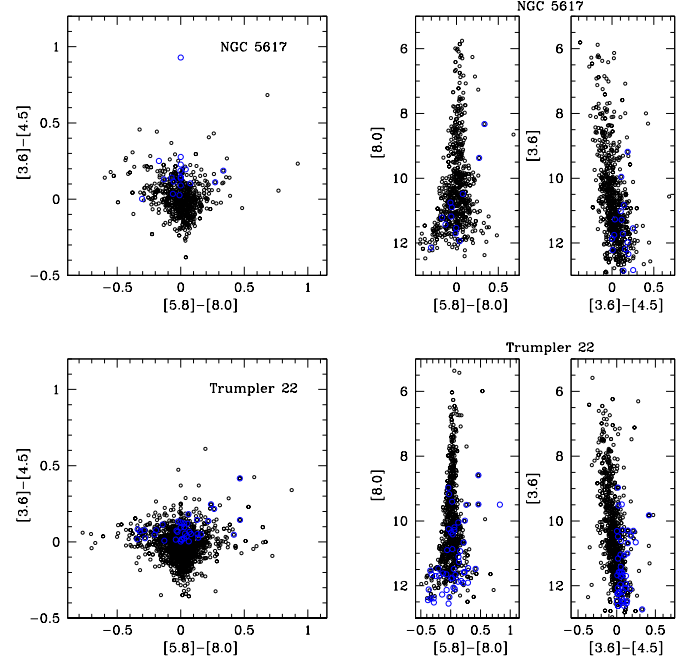


Figure 17. (Top left panel) $[5.8]-[8.0]$ vs $[3.6]-[4.5]$ color-color diagram for NGC 5617. (Top right panel) $[8.0],[5.8]-[8.0]$ and $[3.6],[3.6]-[4.5]$ CMDs for NGC 5617. Same as Trumpler 22 in bottom panels. Blue dots are young stellar objects as identified towards the cluster region.

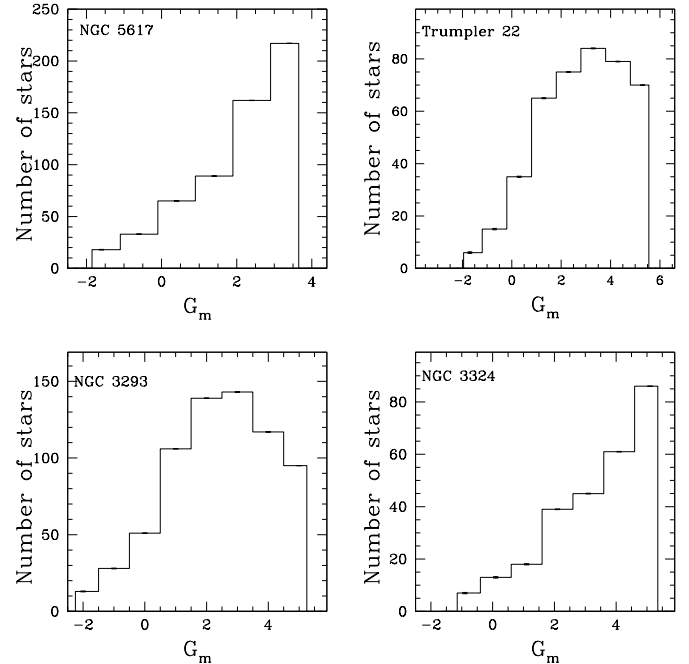


Figure 18. Luminosity function of main sequence stars in the region of the clusters NGC 5617, Trumpler 22, NGC 3293 and NGC 3324

Table 7. Various fundamental parameters of the clusters NGC 5617, Trumpler 22, NGC 3293 and NGC 3324.

Parameter	NGC 5617	Trumpler 22	NGC 3293	NGC 3324
RA(deg)	217.45 ± 0.008	217.82 ± 0.006	158.95 ± 0.007	159.35 ± 0.01
DEC(deg)	-60.72 ± 0.002	-61.16 ± 0.004	-58.23 ± 0.004	-58.62 ± 0.003
Radius(arcmin)	3.5	5.5	6.5	5.5
Radius(parsec)	2.6	4.3	5.0	4.5
$\mu_{\alpha} \cos \delta (mas \ yr^{-1})$	-5.66 ± 0.01	-5.13 ± 0.01	-7.65 ± 0.01	-7.06 ± 0.01
$\mu_{\delta} (mas \ yr^{-1})$	-3.19 ± 0.01	-2.70 ± 0.01	3.36 ± 0.009	2.85 ± 0.01
Parallax(mas)	0.41 ± 0.008	0.38 ± 0.009	0.39 ± 0.004	0.36 ± 0.1
Age(Myr)	90 ± 10	90 ± 10	12 ± 3	12 ± 3
Metal abundance	0.019	0.019	0.019	0.019
E(J-H) (mag)	0.17 ± 0.03	0.20 ± 0.03	0.07 ± 0.02	0.14 ± 0.03
E(J-K) (mag)	0.32 ± 0.05	0.39 ± 0.06	0.15 ± 0.05	0.31 ± 0.07
E(B-V) (mag)	0.55 ± 0.05	0.64 ± 0.05	0.23 ± 0.03	0.45 ± 0.05
R_V	~ 3.1	~ 3.1	~ 4	~ 2
Distance modulus (mag)	13.70 ± 0.40	14.20 ± 0.30	12.90 ± 0.20	13.00 ± 0.20
Distance (Kpc)	2.43 ± 0.08	2.64 ± 0.07	2.59 ± 0.10	2.80 ± 0.2
X(Kpc)	-2.30	-2.60	0.70	0.78
Y(Kpc)	7.85	7.83	-2.50	-2.71
Z(Kpc)	-0.004	-0.020	0.003	-0.007
R_{GC} (Kpc)	10.90 ± 0.5	11.20 ± 0.8	7.9 ± 0.4	8.0 ± 0.3
Total Luminosity(mag)	~ 3.4	~ 3.3	~ 3.3	~ 5.2
Cluster members	584	429	692	273
MF slope	1.40 ± 0.16	1.44 ± 0.24	1.59 ± 0.22	1.51 ± 0.25
Total mass (M_{\odot})	~ 1230	~ 755	~ 1457	~ 580
Average mass(M_{\odot})	2.10	1.76	2.10	2.12
Relaxation time(Myr)	13.5	24.5	26	17
Dynamical evolution parameter (τ)	~ 6.5	~ 3.7	~ 0.46	~ 0.7

database. The diagrams show that the interstellar extinction law is normal towards the cluster's area of NGC 5617 and Trumpler 22. We found extinction law is abnormal for clusters NGC 3293 and NGC 3324.

(iii) The distance estimation from parallax are well supported by the values estimated using the isochrone fitting method to the clusters CMDs. We obtained a similar age of cluster pairs by comparing with the theoretical isochrones of solar metallicity taken from Marigo et al. (2017).

(iv) We obtained 18 and 44 stars towards the cluster region of NGC 5617 and Trumpler 22 as the YSOs reddening parameter (Q) method.

(v) We determined LFs and MFs of both objects by considering the members as selected on the basis of membership probability of stars. The MF slopes are in fair agreement with the Salpeter (1955) value for the clusters under study.

(vi) The presence of mass-segregation is examined for these clusters using probable cluster members. We found that the massive stars are concentrated towards the inner regions of the clusters in comparison to faint stars. The confidence level of mass segregation is found as 88 %, 75 %, 77 % and 70 % for NGC 5617, Trumpler 22, NGC 3293 and NGC 3324, respectively on the basis of the K-S test. Our study indicates that NGC 5617 and Trumpler 22 are dynamically relaxed while NGC 3293 and NGC 3324 are not relaxed.

(vii) Galactic orbits and orbital parameters are estimated using Galactic potential models. We found that these objects are orbiting in a boxy pattern in circular orbit. The different orbital parameters are listed in Table 1 and 2 for the clus-

ters under study. Present analysis shows that clusters (NGC 5617 and Trumpler 22) and (NGC 3293 and NGC 3324) are physically connected and are cluster pairs of Milky Way.

10 ACKNOWLEDGEMENTS

The authors are thankful to the anonymous referee for useful comments, which improved the contents of the paper significantly. This work has been financially supported by the Natural Science Foundation of China (NSFC-11590782, NSFC-11421303). Devesh P. Sariya and Ing-Guey Jiang are supported by the grant from the Ministry of Science and Technology (MOST), Taiwan. The grant numbers are MOST 105-2119-M-007 -029 -MY3 and MOST 106-2112-M-007 -006 -MY3. This work has made use of data from the European Space Agency (ESA) mission Gaia (<https://www.cosmos.esa.int/gaia>), processed by the Gaia Data Processing and Analysis Consortium (DPAC, <https://www.cosmos.esa.int/web/gaia/dpac/consortium>). Funding for the DPAC has been provided by national institutions, in particular the institutions participating in the Gaia Multilateral Agreement. In addition to this, It is worth to mention that, this work has been done by using WEBDA.

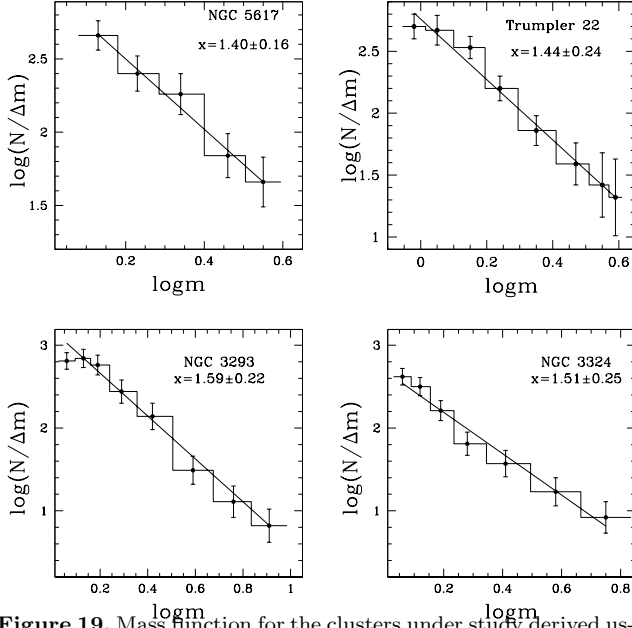


Figure 19. Mass function for the clusters under study derived using probable cluster members and Marigo et al. (2017) isochrones. The error bars represent $\frac{1}{\sqrt{N}}$.

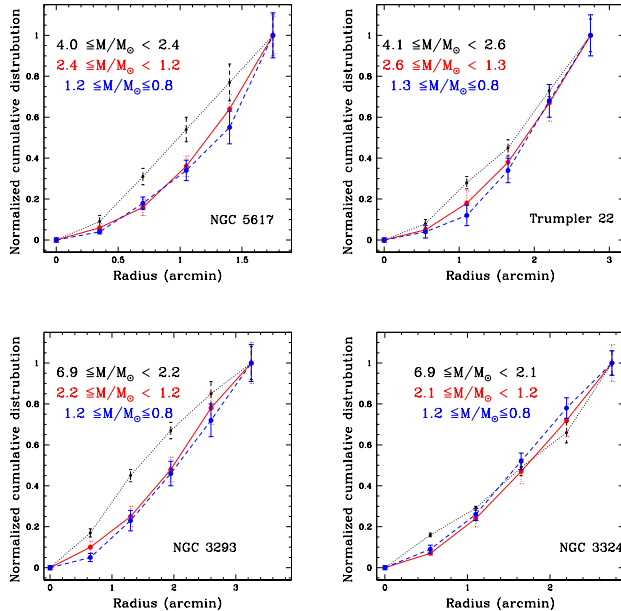


Figure 20. The cumulative radial distribution for NGC 5617, Trumpler 22, NGC 3293 and NGC 3324 in various mass range.

11 DATA AVAILABILITY

We have used the different data sets for the analysis of two pairs of binary clusters (NGC 5617 and Trumpler 22) and (NGC 3293 and NGC 3324), which are publicly available as following,

- GAIA EDR3

<https://vizier.u-strasbg.fr/viz-bin/VizieR-3?-source=I/350/gaiaedr3>

<https://vizier.u-strasbg.fr/viz-bin/VizieR-3?-source=II/311/wise>

- WISE

<https://vizier.u-strasbg.fr/viz-bin/VizieR-3?-source=II/311/wise>

<https://vizier.u-strasbg.fr/viz-bin/VizieR-3?-source=II/348>

- VVV

<http://vizier.u-strasbg.fr/viz-bin/VizieR?-source=II/348>

- APASS

<http://vizier.u-strasbg.fr/viz-bin/VizieR?-source=II>

- GLIMPSE

<https://vizier.u-strasbg.fr/viz-bin/VizieR?-source=>

- VPHAS

<http://vizier.u-strasbg.fr/viz-bin/VizieR?-source=II>

REFERENCES

- Ahumada, J. & Lapasset, E. 2007, *A&AS*, 463, 789
- Allen, C. & Santillan, A. 1991, *Rev. Mexicana Astron. Astrofis.*, 22, 255
- Arenou, F., Luri, X., Babusiaux, C. et al. 2018, *A&A*, 616, A17
- Bajkova, A. T. & Bobylev, V. V. 2016, *Astronomy Letters*, 42, 9
- Balaguer-Núñez L., Tian, K. P., Zhao, J. L., 1998, *A&AS*, 133, 387
- Bailer-Jones C. A. L., Rybizki J., Foesneau M., Mantelet G., Andrae R., 2018, *AJ*, 156, 58
- Bate, M. R., Bonnell, I. A. & Bromm, V. 2003, *MNRAS*, 339, 577
- Baume, G. et al., 2003, *A&A*, 402 549B
- Becker, W. & Fenkart, R. 1971, *A&AS*, 4, 241
- Bellini A., Piotto G., Bedin L. R., et al., 2009, *A&A*, 493, 959
- Benjamin R. A. et al., 2003, *PASP*, 115, 953
- Bhatia R. K., 1990, *PASJ*, 42, 757
- Bhatia R. K., Hatzidimitriou D., 1988, *MNRAS*, 230, 215
- Bisht, D., Yadav, R. K. S. & Durgapal, A. K. 2017, *NewA*, 52, 55B
- Bisht, D., Yadav, R. K. S., Ganesh, S., Durgapal, A. K., Rangwal, G. & Fynbo, J. P. U. 2019, *MNRAS*, 482, 1471B
- Bisht, D., Zhu, Qingfeng., Yadav, R. K. S., Durgapal, Alok., Rangwal, Geeta., 2020, *MNRAS*, 494, 607-623
- Bisht, D., W. H. Elsanhoury., Zhu, Qingfeng., et al., 2020, *The Astronomical Journal*, 160, 119
- Binney J., Tremaine S., 2008, *Galactic Dynamics*. Princeton Univ. Press, Princeton, NJ
- Bobylev, V. V., Bajkova, A. T. & Gromov, A. O. 2017, *Astronomy Letters*, 43, 4
- Bonatto, C. & Bica, E. 2009, *MNRAS*, 397, 1915
- Brandl, B., et al. 1996, *ApJ*, 466, 254
- Buckner A. S. M., Froebrich D., 2013, *MNRAS*, 436, 1465
- Cantat-Gaudin, T., Jordi, C., Vallenari, A., et al. 2018, *A&A*, 618A, 93C
- Cantat-Gaudin T., et al., 2019, *A&A*, 624, A126
- Caldwell, J. A. R., Cousins, A. W. J., Ahlers, C. C., van

- Wamelen, P. & Maritz, E. J. 1993, South Astronomical Observatory, Circ No. 15
- Carraro G., Patat F., Baumgardt, H., 2001, *A&A*, 371, 107C
- Carraro G., Villanova S., Demarque P., Moni Bidin C., McSwain M. V., 2008, *MNRAS*, 386, 1625
- Carraro G., Chiosi C., 1994b, *A&A*, 288, 751
- Cardelli, J. A., Clayton, G. C. & Mathis, J. S. 1989, *ApJ*, 345, 245
- Castro-Ginard A., et al., 2020, arxiv e-prints, p.arXiv:2001.07122
- Chen, W. P., Chen, C. W., & Shu, C. G. 2004, *AJ*, 128, 2306
- Chumak Y. O., Platais I., McLaughlin D. E., Rastorguev A. S., Chumak O. V., 2010, *MNRAS*, 402, 1841
- Converse J. M., Stahler S. W., 2011, *MNRAS*, 410, 2787
- Churchwell E. et al., 2004, *ApJS*, 154, 322
- Claria, J. J., 1977, *A&AS*, 27, 145C
- Dalton, G. B. et al., 2006, *SPIE*, 6269E, 0XD
- de la Fuente Marcos R., de la Fuente Marcos C., 2010, *ApJ*, 719, 104
- De Silva, G. M. et al., 2015, *MNRAS*, 453, 106D
- Delgado, A. J., Alfaro, E. J., Yum, J. L., 2011, *A&A*, 531A, 141D
- Dias, W. S., Alessi, B. S., Moitinho, A., Lepine, J. R. D., 2002, *A&A*, 389, 871
- Dib S., Schmeja., Hony S., 2017, *MNRAS*, 464, 1738
- Dieball A., Grebel E. K., 2000, *A&A*, 358, 897
- Dieball A., Muller H., Grebel E. K., 2002, *A&A*, 391, 547
- Drew, J. E. et al., 2014, *MNRAS*, 440, 2036D
- Dutra, C., Santiago, B. & Bica, E. 2002, *A&A*, 381, 219
- Friel E. D., Janes K. A., 1993, *A&A*, 267, 75
- Fiorucci M., Munari U., 2003, *A&A*, 401, 781
- Evans, D. W., Riello, M., De Angeli, F., et al. 2018, *A&A*, 616, A4
- Gaia Collaboration et al., 2016a, *A&A*, 595, A1
- Gaia Collaboration et al., 2016b, *A&A*, 595, A2
- Gaia Collaboration et al. 2018a, *A&A*, 616, A10
- Gaia Collaboration et al. 2018b, *A&A*, 616, A17
- Genzel, R. & Townes, C. H. 1987, *ARA&A*, 25, 377
- Girard, T. M., Grundy, W. M., Lopez, C. E., & van Altena, W. F. 1989, *AJ*, 98, 227
- Harris W. E., Pudritz R. E., 1994, *ApJ*, 429, 177
- Haug U., 1978, *A&AS*, 34, 417
- Henden, A., Munari, U. 2014, *Contrib. Astron. Obs. Skalnate Pleso*, 43, 518
- Heden, A., Templeton, M., Terrell, D., et al. 2016, *VizieR Online Data Catalog*, II/336
- Hendy, W. H. M. 2018, *NRIAG Journal of Astronomy and Geophysics*, 7, 180-186
- Hillenbrand L. A., Hartmann L. W., *ApJ*, 492, 540
- Johnson D. R. H., Soderblom D. R., 1987, *AJ*, 93, 864
- Jose, J., Herczeg, G. J., Samal, M. R., Fang, Q., & Panwar, N. 2017, *ApJ*, 836, 98
- Joshi Y. C., Balona L. A., Joshi S., KUMAR B., 2014, *MNRAS*, 437, 804
- Joshi Y. C., Maurya J., John A. A., Panchal A., Joshi S., Kumar B., 2020, *MNRAS*, 492, 3602
- Kjeldsen, H. & Frandsen, S. 1991, *A&AS*, 87, 119
- King, I. 1962, *AJ*, 67, 471
- Kim, S. S., Figger, D. F., Lee, H. M. & Morris, M. 2000, *ApJ*, 545, 301
- Lada C. J., Lada, E. A., 1991, in Jones K., ed., *ASP Conf. Ser.*, Vol. 13, The formation and evolution of star clusters, Astron. Soc. Pac., San Francisco, p.3
- Larsen S. S., 2006, *An ISHAPE Users Guide*. p. 14
- Lindegren, L., Hernandez, J., Bombrun, A, et al. 2018, *A&A*, 616, A2
- Lindoff U., 1968, *Ark. Astron.*, 4, 493
- Luri X., et al., 2018, *A&A*, 616, A9
- Maciejewski, G. & Niedzielski, A. 2007, *A&A*, 467, 1065
- Marigo, P. et al. 2017, *ApJ*, 835, 77
- Meylan, G., 2000, Massive stellar clusters, conference held in strasbourg, france. In: Lanon, A., Boily, C. (Eds.), *Astronomical Society of the Pacific Conference Series*, p.215
- Minniti, D., Lucas, P. W., Emerson, J. P, et al. 2010, *NewA*, 15, 433
- Peterson, C. J. & King, I. R. 1975, *AJ*, 80, 427
- Preibisch, T et al., 2017, *A&A*, 605A, 85P
- Rangwal, G., Yadav, R. K. S., Durgapal, A., Bisht, D. & Nardiello, D. 2019, *MNRAS*, 490, 1383
- Reid M. J., Brunthaler A. 2004, *ApJ*, 616, 872
- Riess A. G., et al., 2018, *ApJ*, 861, 126
- Romanishim W., Angel J. R. P., 1980, *ApJ*, 235, 992
- Saito, R. K., Hempel, M., Minniti, D., et al. 2012b, *A&A*, 537, A107
- Salpeter, E. E. 1955, *ApJ*, 121, 161
- Sariya, D. P., & Yadav, R. K. S. 2015, *A&A*, 584, A59
- Sariya, D. P., Jiang, Ing-Guey., Sizova, M. D., et al. 2021a, *AJ*, 161, 101
- Sariya, D. P., Jiang, Ing-Guey., Bisht, D., et al. 2021b, *AJ*, 161, 102
- Schlegel D. J., Finkbeiner D. P., Davis M., 1998, *ApJ*, 500, 525
- Schonrich, Ralph., Binney, James., Dehnen, Walter. 2010, *MNRAS*, 403, 1829S
- Shao Z., Zhao J., 1996, *Acta Astronomica Sinica*, 37, 377
- Sharma, S., Pandey, A. K., Ogura, K., et al. 2008, *AJ*, 135, 1934
- Sharma, S., Pandey, A. K., Ojha, D. K., et al. 2017, *MNRAS*, 467, 2943
- Soubiran et al. 2018, *A&A*, 623C, 2S
- Spitzer, L. & Hart, M. 1971, *ApJ*, 164, 399
- Slawson, Robert W., Ninkov, Zoran., Horch, Elliot., 2007, *Ap&SS*, 312, 171S
- Subramaniam A., Gorti U., Sagar R., Bhatt H. C., 1995, *A&A*, 302, 86
- Tuvikene, T., Sterken C., 2006, *ASPC*, 349, 359T
- von Hoerner S., 1957, *ApJ*, 125, 451
- Wilkinson, M. I. & Evans, N. W. 1999, *MNRAS*, 310, 645
- Wright, E. L., Eisenhardt, P. R. M., Mainzer, A. K., Ressler, M. E., Cutri, R. M., Jarrett, T., Kirkpatrick, J. D. & Padgett, D. 2010, *AJ*, 140, 1868
- Wang, S. & Chen, X., 2019, *ApJ*, 877, 116W
- Webb J. J., Sills A., Harris W. E., Hurley J. R., 2014, *MNRAS*, 445, 1048
- Wu, Z. Y., Zhou, X., Ma, J. & Du, C. H. 2009, *MNRAS*, 399, 2146
- Yadav R. K. S., Bedin L. R., Piotto G., et al., 2008, *A&A*, 484, 609
- Yadav R. K. S., Sariya D. P., Sagar R., 2013, *MNRAS*, 430, 3350